

Electronic Supplementary Information for:

**An Experimental and Theoretical Study of the Magnetic Relaxation in Heterometallic Coordination Polymers Based on 6-methyl-2-oxonicotinate and Lanthanide(III) Ions with Square Antiprismatic Environment**

Laura Razquin-Bobillo,<sup>a</sup> Oier Pajuelo-Corral,<sup>a</sup> Andoni Zabala-Lekuona,<sup>a</sup> Antonio Rodríguez-Díéguez<sup>b</sup> and Javier Cepeda\*,<sup>a</sup>

<sup>a</sup> Departamento de Química Aplicada, Facultad de Química, Universidad del País Vasco (UPV/EHU), 20018 Donostia, Spain. <sup>b</sup> Departamento de Química Inorgánica, UEQ, C/ Severo Ochoa s/n, Universidad de Granada, 18071, Granada, Spain.

Contents:

- S1. Thermal characterization of compounds.
- S2. FT-IR spectroscopy.
- S3. Powder X-ray diffraction analysis of as-synthesized compounds.
- S4. Continuous shape measures of compound **1<sub>Dy</sub>**.
- S5. *Dc* susceptibility measurements.
- S6. Magnetic *ac* measurements.
- S7. Additional figures of the crystal structure.
- S8. References.

## S1. Thermal characterization of compounds.

The thermal behaviour of compound  $\mathbf{1}_{\text{Dy}}$  has been studied as a representative compound for all compounds by means of thermogravimetric/differential thermal analyses (TG/DTA) in order to further confirm the purity of the polycrystalline samples. As it can be seen in Figure S1, when the compounds are heated above room temperature, they show a small mass loss which is assigned to eight water molecules. Above 300 °C, the compounds undergo two exothermic processes as a consequence of the decomposition of organic matter, where the final product is  $\text{Dy}_2\text{O}_3$  (1/2) +  $\text{Na}_2\text{O}$  (1/2).

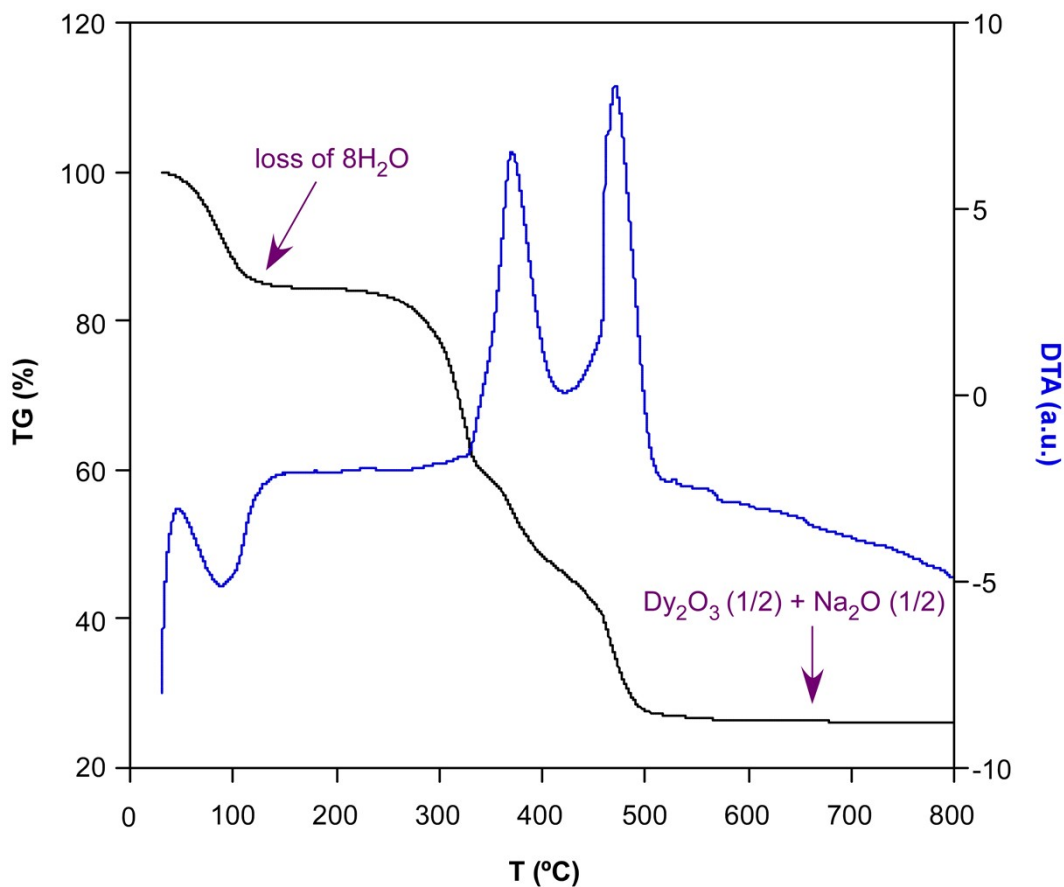


**Figure S1.** TG/DTA curves of compound  $\mathbf{1}_{\text{Dy}}$ .

## S2. FT-IR spectroscopy.

Infrared spectroscopy has been used for the initial characterization of the compounds, as it allows us to check whether the synthesized complexes contain the ligand and whether it is coordinated to the metals. The spectra obtained for complexes **1<sub>Dy</sub>** and **2<sub>Er</sub>** show a similar structure (Figure S2), which can be considered as the result of the ligand exhibiting the same tautomeric form in all compounds. In this sense, it should be mentioned that although the coordination mode of the ligand in its tautomer 1H-2-oxo-6-methyl-nicotinate is variable, in all compounds a chelate ring is generated between the ketone and carboxylate groups, imposing the main similarity of the infrared spectra (presence of most of the bands).

In all spectra, the first band appearing between 3500-3300 cm<sup>-1</sup> corresponds to the vibrational stress of the O-H bonds of the adsorbing water molecules in the samples by ambient humidity (in the case of the free ligand) or of the water molecules of crystallization. This band is followed by a second broader band between 3300-2300 cm<sup>-1</sup>, which corresponds to the vibrations of the O-H, N-H and C-H bonds of the ligand. It is significant that in the ligand spectrum this band is much more intense than with the compounds, as the inter- and intra-molecular hydrogen bonds between the ligand molecules vibrate more intensely. In particular, a robust band of the protonated carboxylate group is seen in the ligand and weak vibrational signals of the N-H and C-H pyridine ring are observed in all compounds. The strong bands appearing in the range 1725-1450 cm<sup>-1</sup> correspond to asymmetric vibrations of the carboxylate group and the C-C and C-N bonds of the aromatic ring, while the symmetric vibrations of the carboxylate group appear in the range 1400-1200 cm<sup>-1</sup>. Again, the spectrum of the free ligand shows a strong broad band between 1725-1665 cm<sup>-1</sup> and narrower at 1508 cm<sup>-1</sup>, an event that corresponds to the protonation of the carboxylate group. It should also be noted that some symmetric vibrations of the carboxylate group are rather impeded in the compounds by the coordination form adopted in the compounds. The remaining bands of smaller wavenumbers can be assigned to the distortions occurring in the aromatic ring, among which Ln-O bonds (Ln = Dy and Er) are also seen.

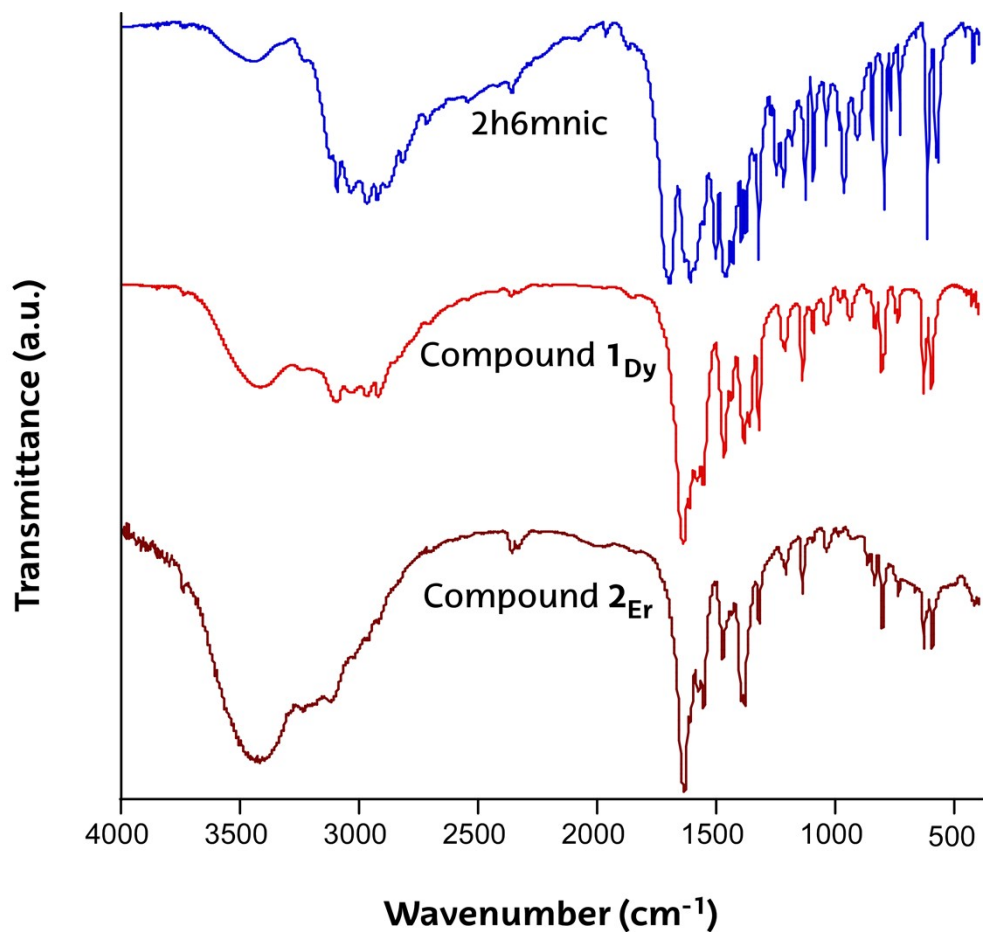


**Figure S2.** IR spectra of 6m2onic and compounds **1<sub>Dy</sub>** and **2<sub>Er</sub>**.

### S3. Powder X-ray diffraction analysis of as-synthesized compounds.

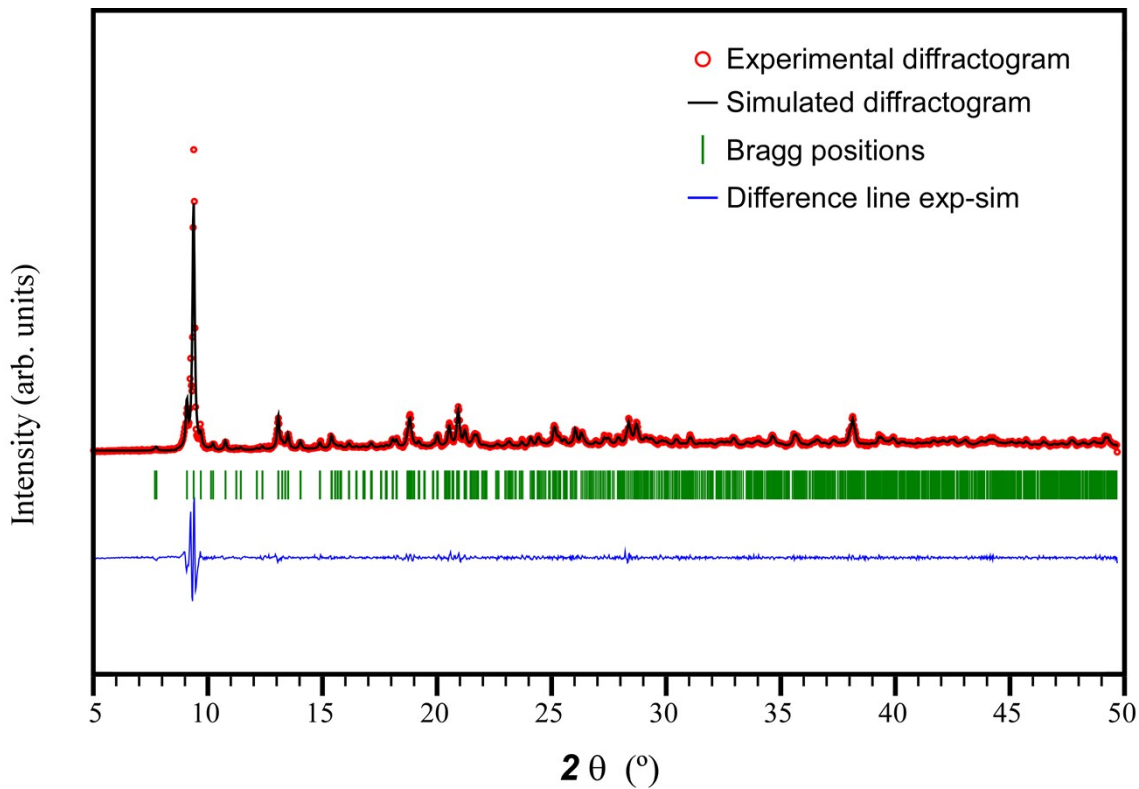


**Figure S3.** Simulated and experimental PXRD of  $\mathbf{1}_{\text{Dy}}$  with the full profile pattern matching analyses.

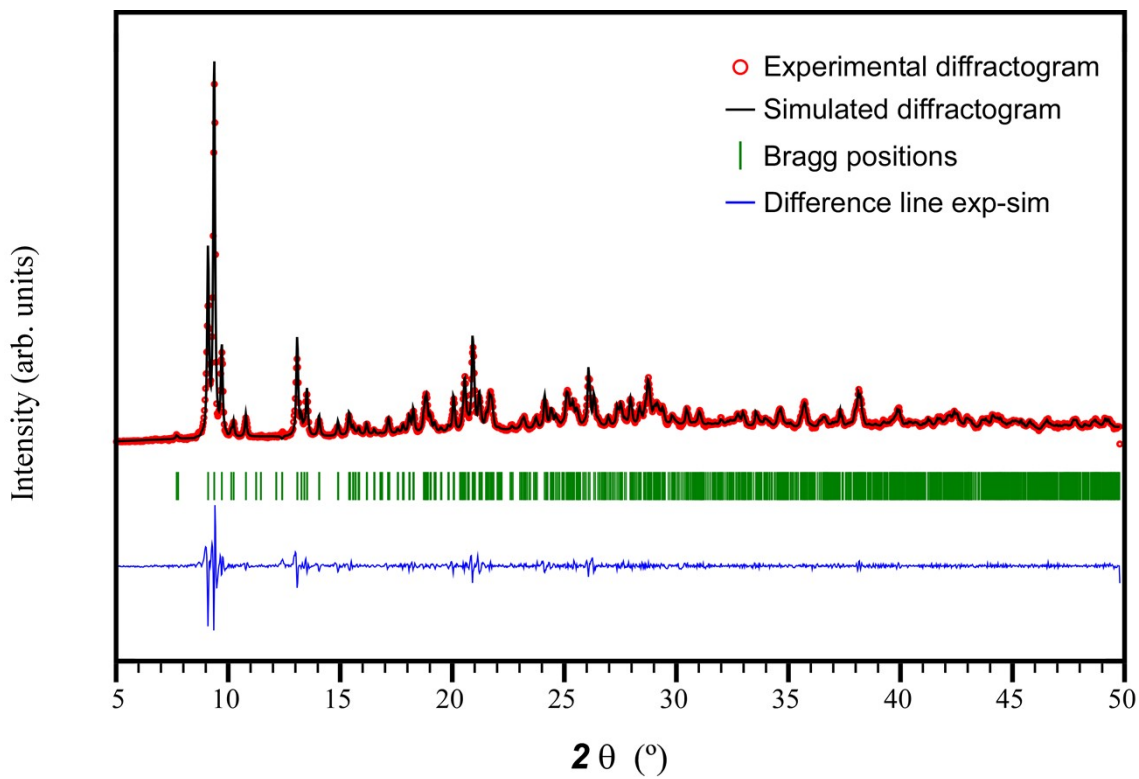


**Figure S4.** Simulated and experimental PXRD of  $\mathbf{2}_{\text{Er}}$  with the full profile pattern matching analyses.

#### S4. Continuous shape measures of compound **1<sub>Dy</sub>**.

**Table S1.** CShMs for the coordination environment of compound **1<sub>Dy</sub>**. The lowest values for each ion are shown highlighted indicating best fits.

Codes:

OP-8	1 D8h	Octagon
HPY-8	2 C7v	Heptagonal pyramid
HBPY-8	3 D6h	Hexagonal bipyramid
CU-8	4 Oh	Cube
SAPR-8	5 D4d	Square antiprism
TDD-8	6 D2d	Triangular dodecahedron
JGBF-8	7 D2d	Johnson gyrobifastigium J26
JETBPY-8	8 D3h	Johnson elongated triangular bipyramid J14
JBTPR-8	9 C2v	Biaugmented trigonal prism J50
BTPR-8	10 C2v	Biaugmented trigonal prism
JSD-8	11 D2d	Snub diphenoïd J84
TT-8	12 Td	Triakis tetrahedron
ETBPY-8	13 D3h	Elongated trigonal bipyramid

Structure [ML8]	1 <sub>Dy</sub> (Dy1)
<b>OP-8</b>	30.867
<b>HPY-8</b>	23.281
<b>HBPY-8</b>	16.478
<b>CU-8</b>	10.017
<b>SAPR-8</b>	<b>0.458</b>
<b>TDD-8</b>	1.992
<b>JGBF-8</b>	15.618
<b>JETBPY-8</b>	28.597
<b>JBTPR-8</b>	2.320

<b>BTPR-8</b>	1.824
<b>JSD-8</b>	4.469
<b>TT-8</b>	10.813
<b>ETBPY-8</b>	24.102

Codes:

HP-6	1 D6h	Hexagon
PPY-6	2 C5v	Pentagonal pyramid
OC-6	3 Oh	Octahedron
TPR-6	4 Oh	Trigonal prism
JPPY-6	5 C5v	Johnson pentagonal pyramid J2

Structure [ML6] 1 <sub>Dy</sub> (Na2)	
<b>HP-6</b>	27.354
<b>PPY-6</b>	15.550
<b>OC-6</b>	<b>6.278</b>
<b>TPR-6</b>	11.442
<b>JPPY-6</b>	19.137

### S5. Dc susceptibility measurements.

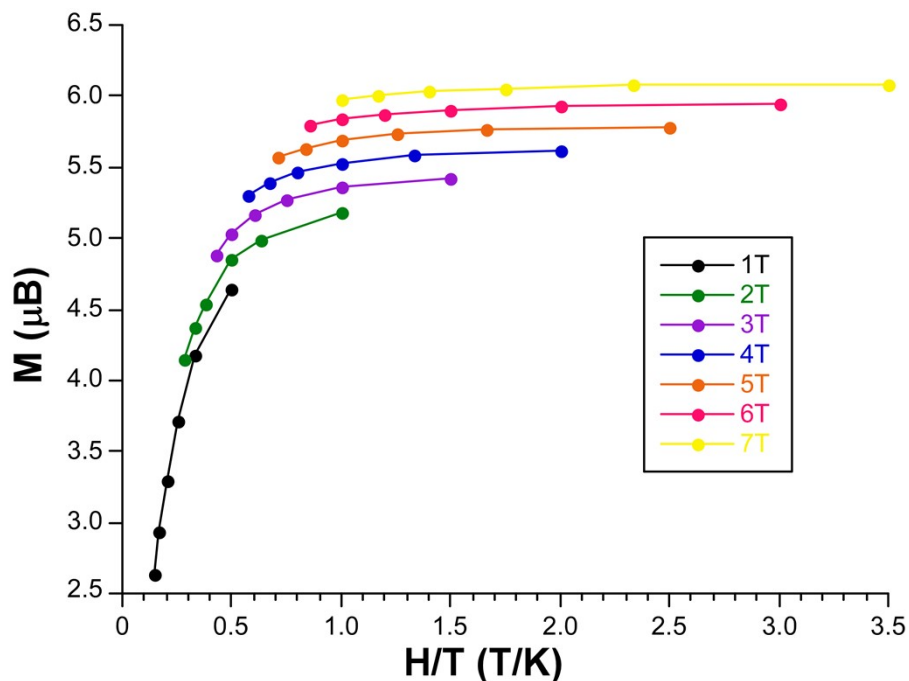


**Figure S5.** Reduced magnetization plot for compound  $\mathbf{1}_{\text{Dy}}$ . The lines are just a guide for the eye.

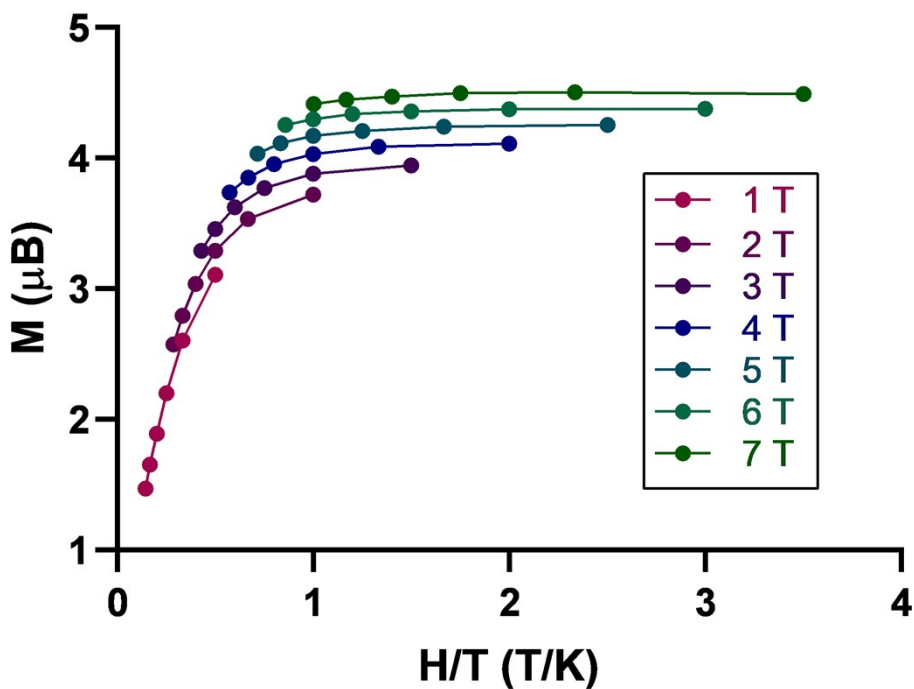


**Figure S6.** Reduced magnetization plot for compound  $\mathbf{2}_{\text{Er}}$ . The lines are just a guide for the eye.

**S6. Magnetic ac measurements.**

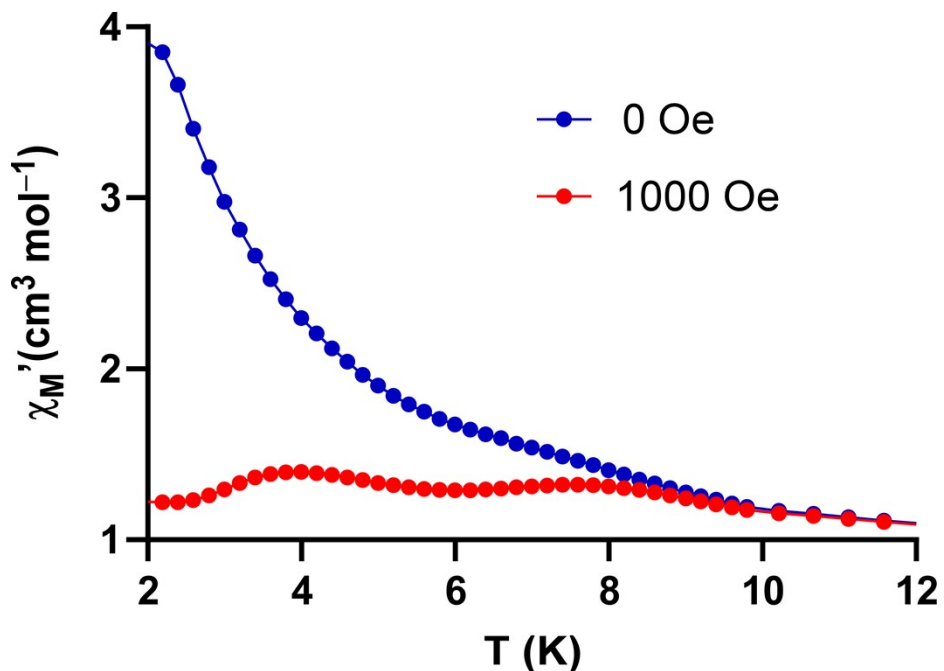


**Figure S7.** Temperature dependence of the in-phase signals of compound  $1_{\text{Dy}}$  recorded at a Freq = 10000 Hz under zero applied *dc* field (blue) and under an applied field of 1000 Oe (red).

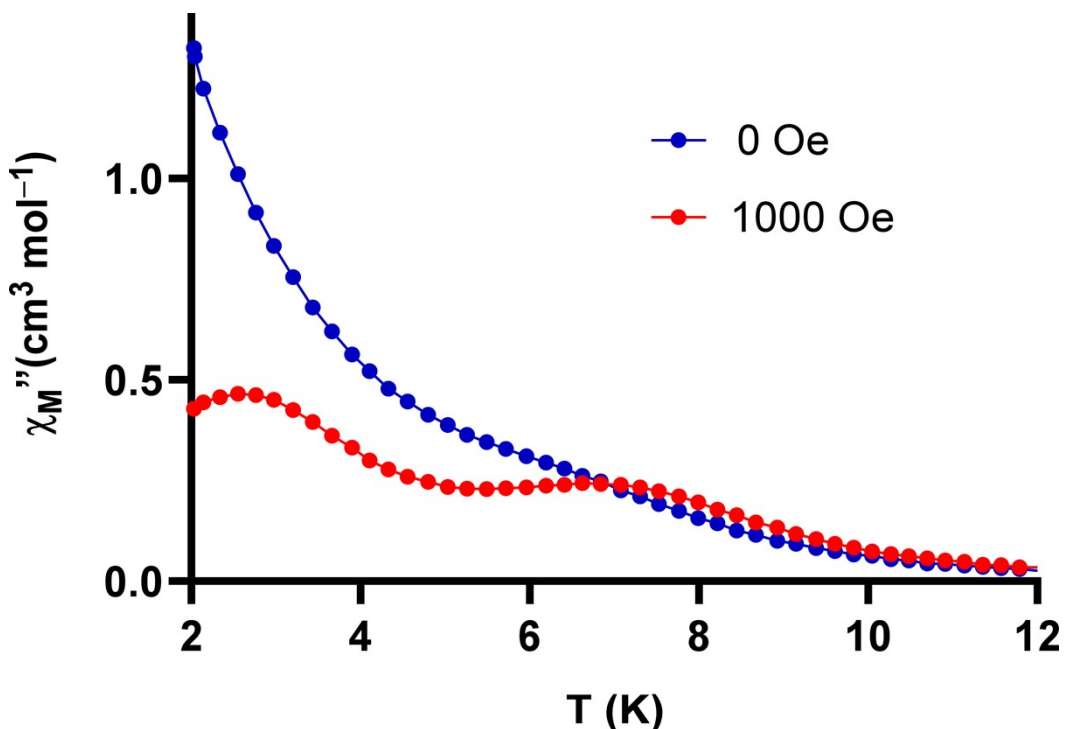


**Figure S8.** Temperature dependence of the out-of-phase signals of compound  $1_{\text{Dy}}$  recorded at a Freq = 10000 Hz under zero applied *dc* field (blue) and under an applied field of 1000 Oe (red).

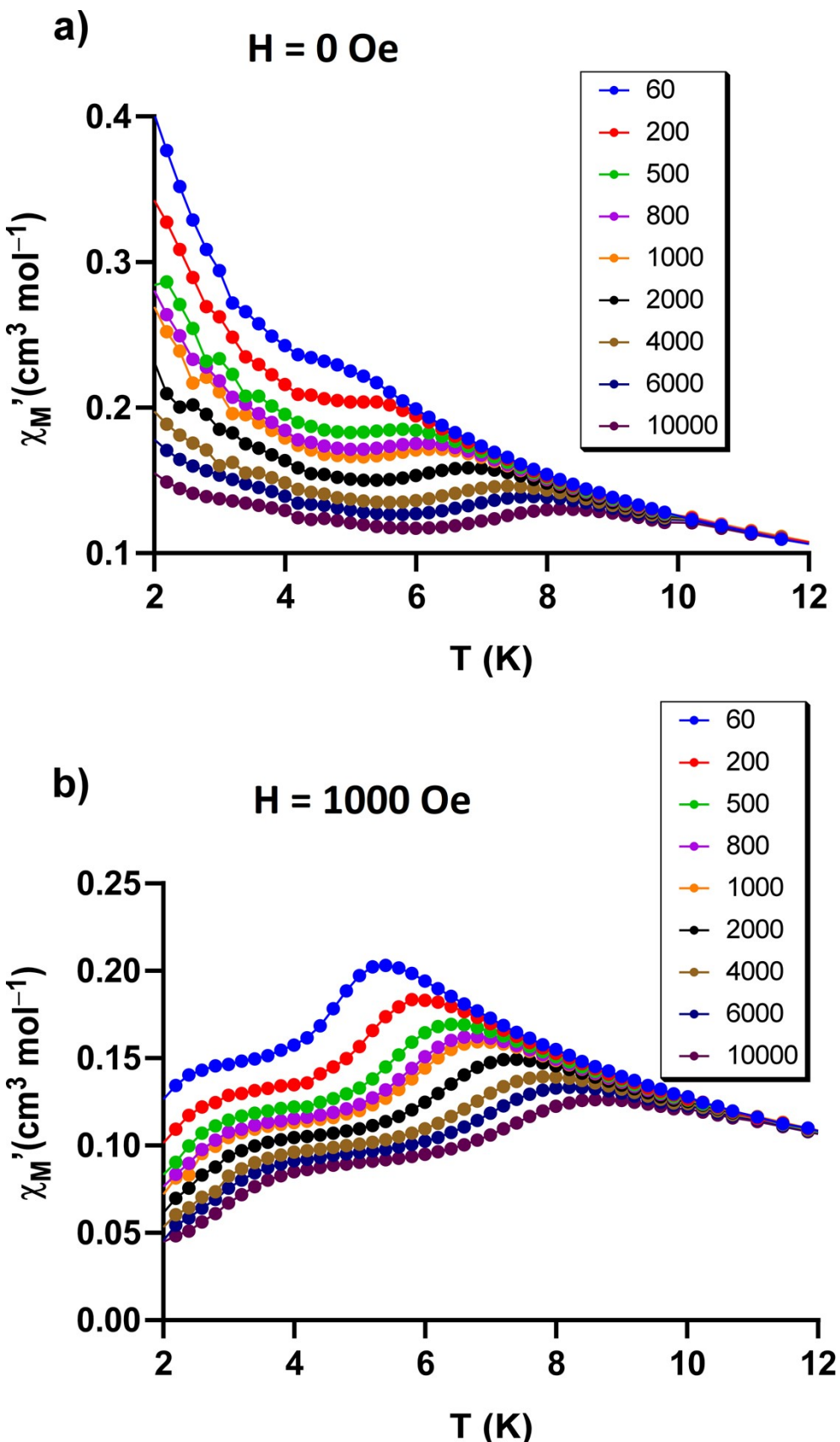
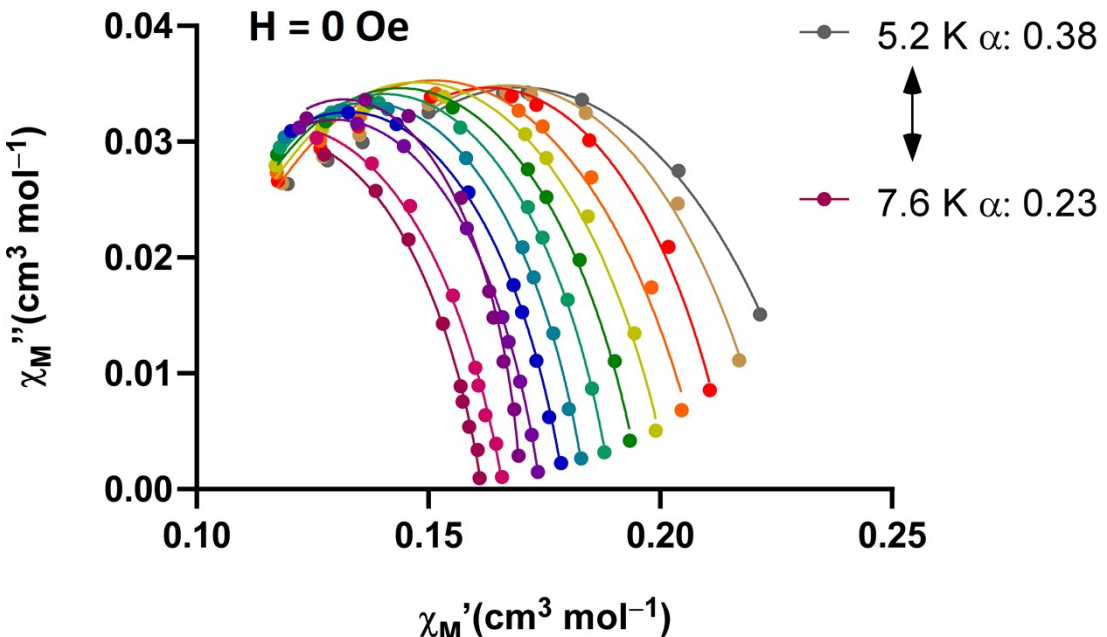


**Figure S9.** Temperature dependence of the in-phase signals of the diluted compound **1<sub>Y/Dy</sub>** at variable frequency (Hz): **a)** under zero applied *dc* field and **b)** under an applied field of 1000 Oe.

a)



b)

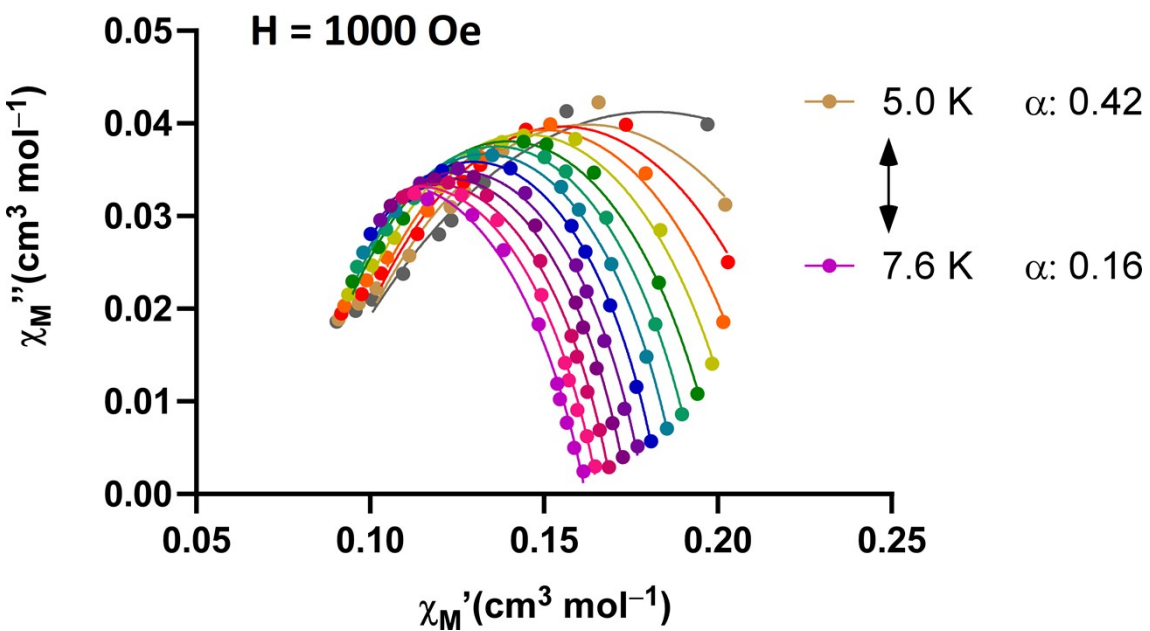


**Figure S10.** Cole-Cole plots for the diluted compound **1<sub>y/Dy</sub>**: **a)** at zero dc field **b)** and under an applied field of 1000 Oe. Solid lines represent the best fit to the generalized Debye model.

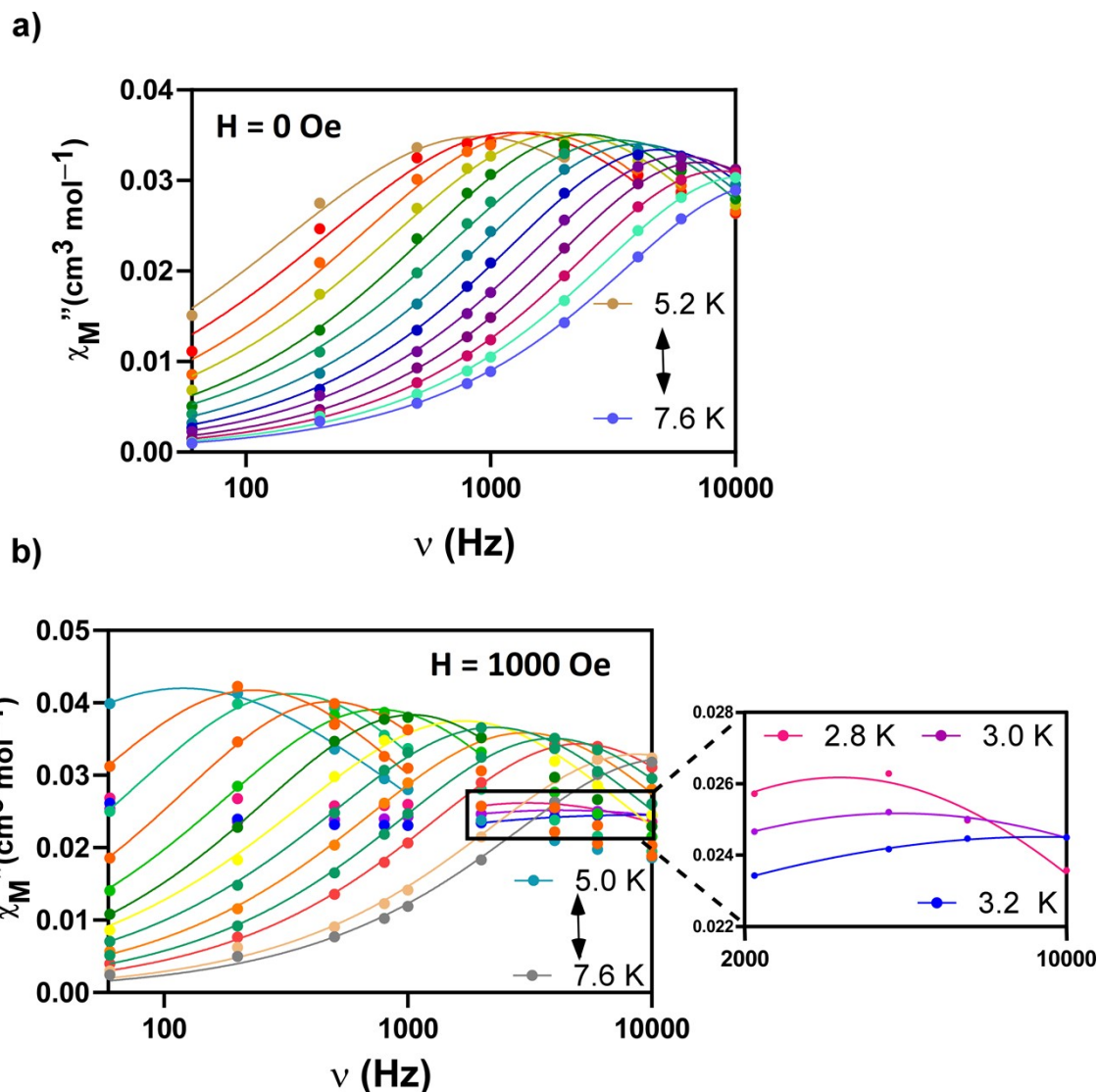


**Figure S11.** Variable-temperature frequency dependence of the  $\chi_M''$  signals for the diluted compound **1<sub>Y</sub>/Dy**: **a)** at zero dc field **b)** and under 1 kOe of applied field. Solid lines represent the best fitting of the experimental data to the Debye model.

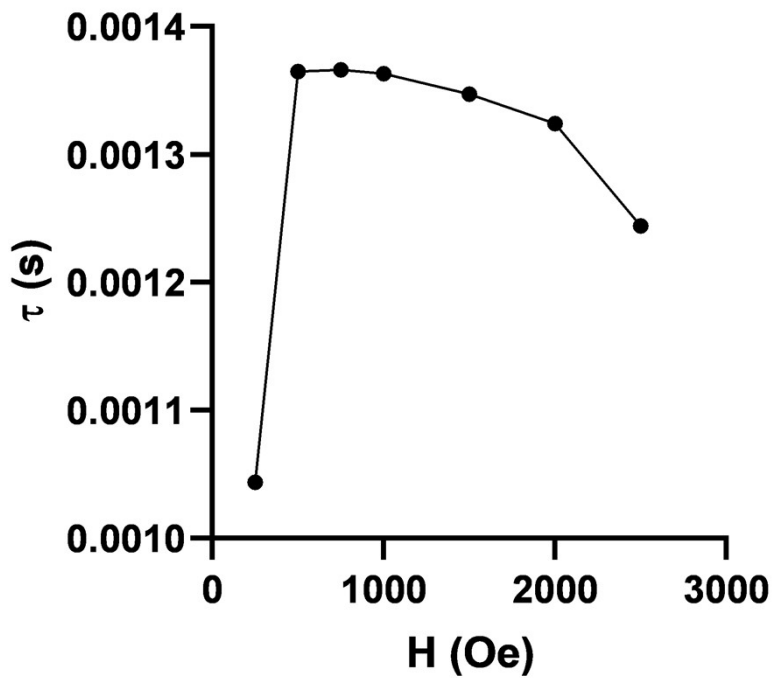


**Figure S12.** Optimization of the  $\text{1}_{\text{Y/Dy}}$  compound field.

**Table S2.** Relaxation Fitting Parameters from Least-Squares Fitting of  $\chi(\phi)$  data for the compound  $\text{1}_{\text{Y/Dy}}$  under an optimal  $H_{dc}$  field of 1000 Oe.

T (K)	FR		SR	
	$\alpha_1$	$\tau_1$ (s)	$\alpha_2$	$\tau_2$ (s)
2.8	0.48	5.14E-05	-	-
3.0	0.63	3.79E-05	-	-
3.2	0.71	1.80E-05	-	-
5.0	-	-	0.42	1.32E-03
5.2	-	-	0.30	6.86E-04
5.4	-	-	0.27	4.81E-04
5.6	-	-	0.24	3.30E-04
5.8	-	-	0.26	2.09E-04
6.0	-	-	0.24	1.53E-04
6.2	-	-	0.29	9.43E-05
6.4	-	-	0.28	7.08E-05
6.6	-	-	0.26	5.29E-05
6.8	-	-	0.24	4.07E-05
7.0	-	-	0.23	3.13E-05
7.2	-	-	0.23	2.43E-05
7.4	-	-	0.24	1.83E-05
7.6	-	-	0.24	1.415E-05

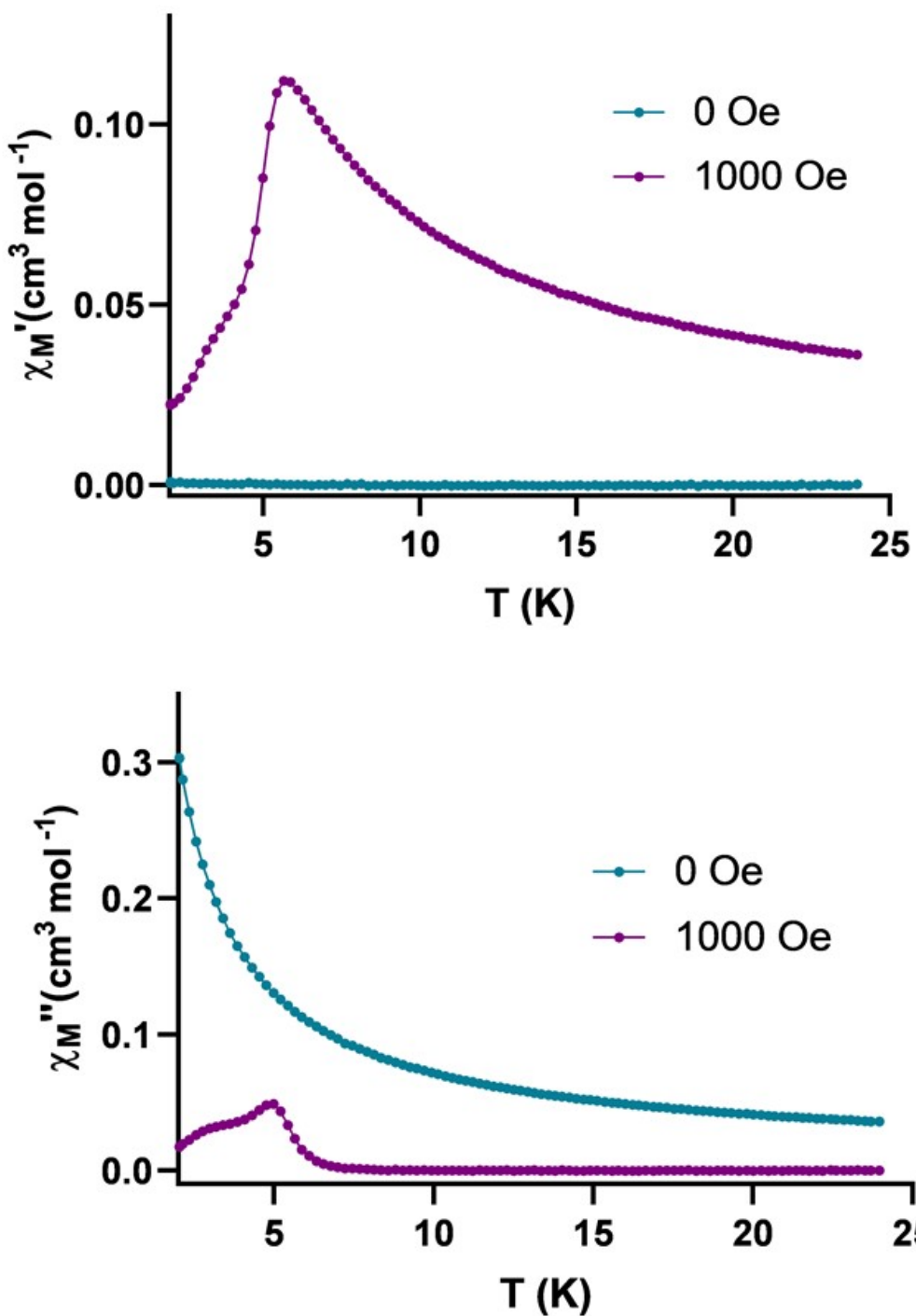


**Figure S13.** Temperature dependence of the in-phase (top) and out-of-phase signals (bottom) of the diluted compound  $\mathbf{2}_{\text{Y/Er}}$  under variable dc fields.

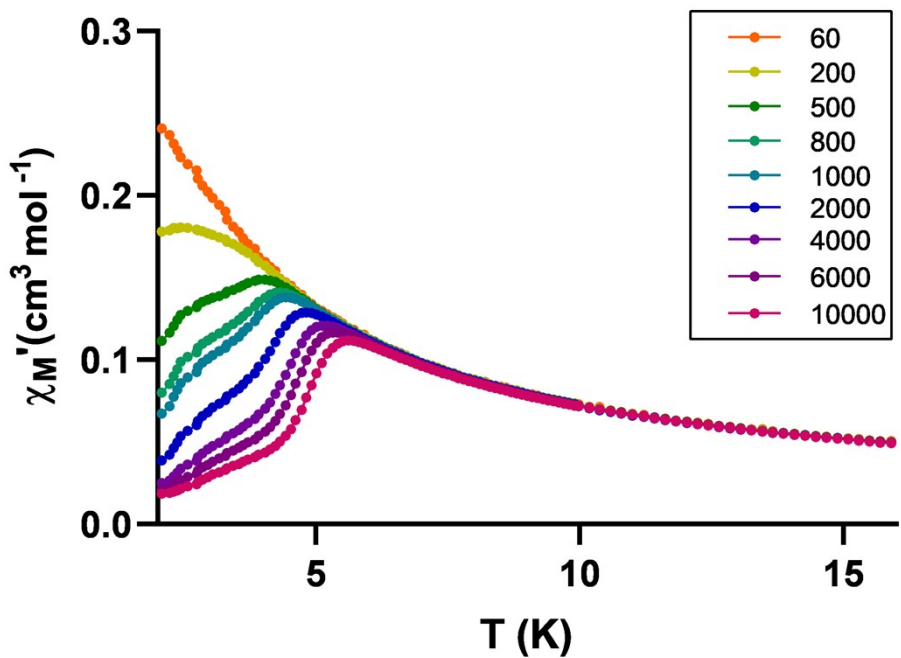


**Figure S14.** Temperature dependence of the in-phase signals of the diluted compound  $2_{Y/Er}$  under the optimum dc field (1500 Oe) and variable frequencies (Hz).

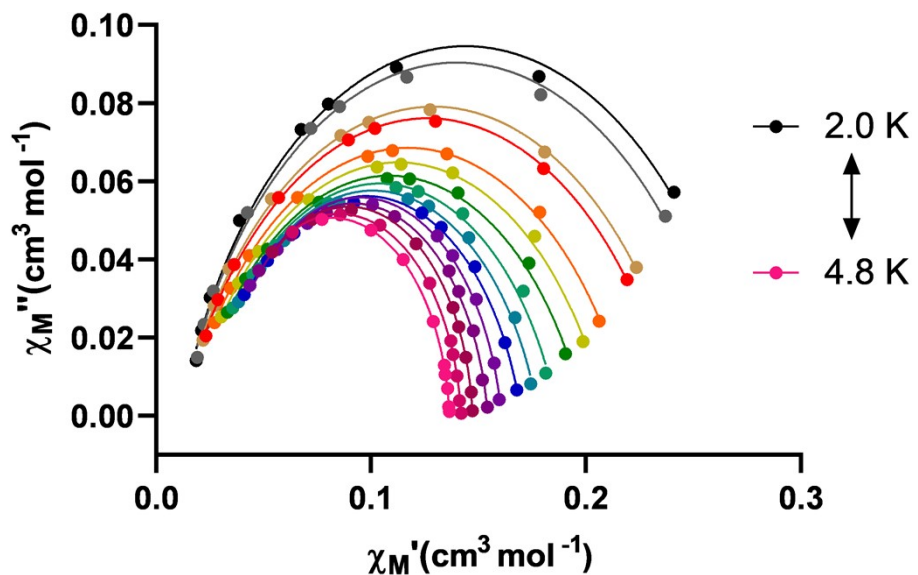


**Figure S15.** Cole-Cole plots for the diluted compound  $2_{Y/Er}$ . Solid lines represent the best fit to the generalized Debye model.

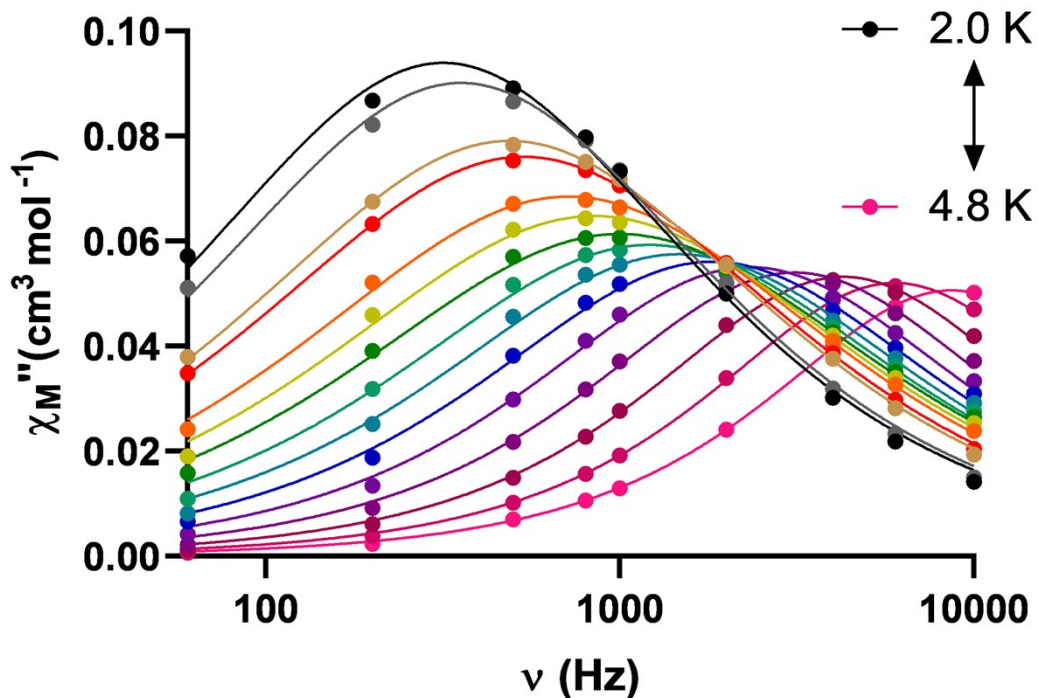


**Figure S16.** Variable-temperature frequency dependence of the  $\chi_M''$  signals for the diluted compound  $2_{\text{Y/Er}}$ . Solid lines represent the best fitting of the experimental data to the Debye model.

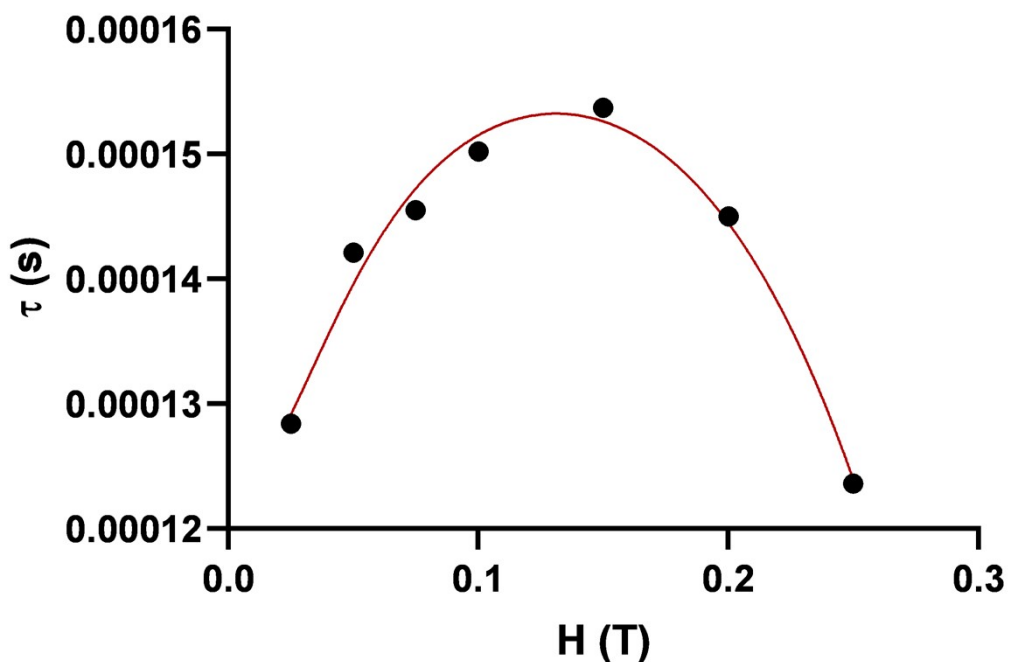


**Figure S17.** Field optimization for diluted compound  $2_{\text{Y/Er}}$ . The red curve is obtained by fitting the data to equation 3 in the main text.

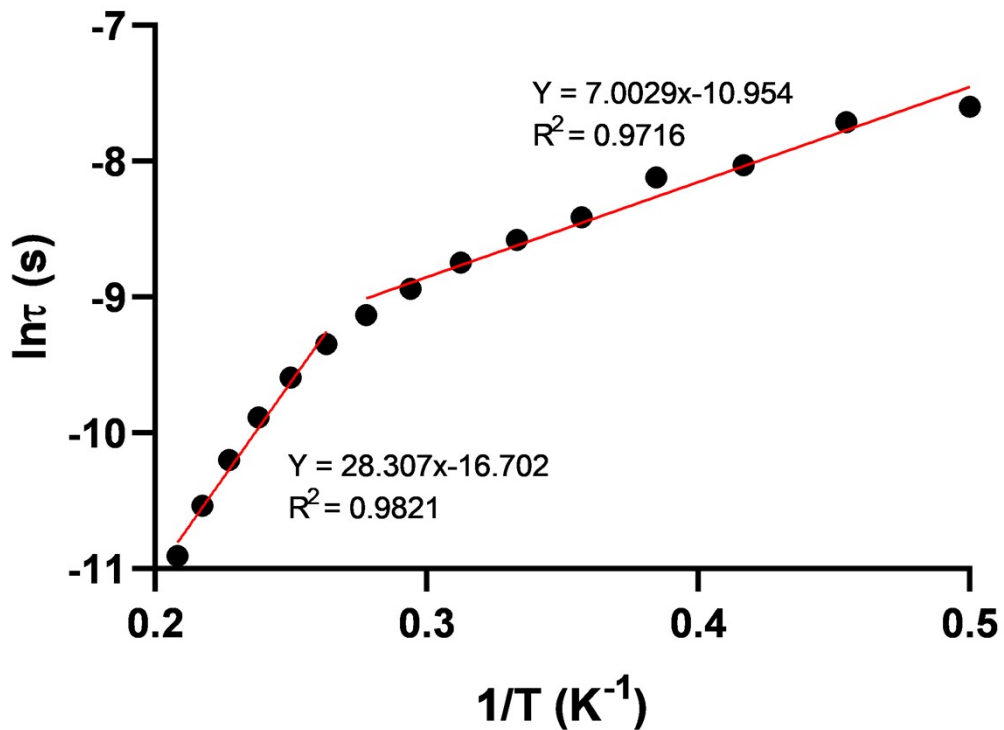


**Figure S18.** The temperature-dependent  $\tau$  distribution in the form of  $\ln(\tau)$  vs  $1/T$  plot for diluted compound  $2_{Y/Er}$ .

**S8. Ab initio calculations.**

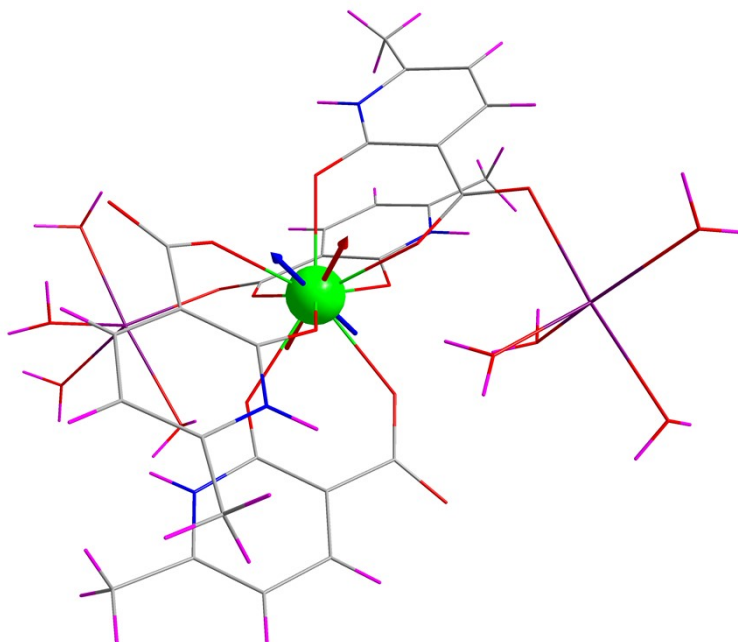


**Figure S19.** View of the Dy(III)-based coordination excerpt used for the *ab initio* calculations on model 5-Dy showing the main calculated magnetic axes of the ground state (blue arrow) and 1<sup>st</sup> excited state (red arrow) Kramers doublets.

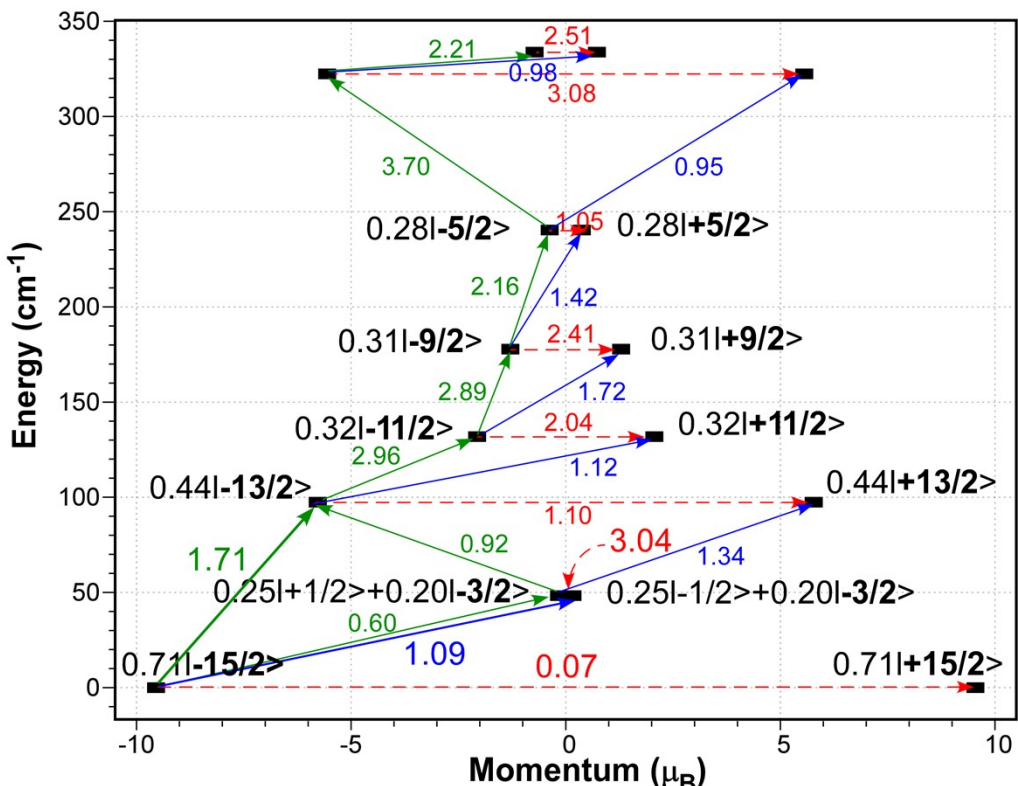


**Figure S20.** *Ab initio* computed relaxation mechanism showing the eight lowest KDs with the main wavefunctions on model 1-Dy (for compound **1<sub>Dy</sub>**). Blue and green lines indicate the relaxation pathways for magnetization reversal mechanism through excited states. The dotted red lines represent the ground state QTM and TA-QTM via excited KDs. The numbers close to each arrow designate matrix elements of transition magnetic moment.

**Table S3.** Energy spectrum and  $g$  tensors for the eight KDs arising from the GS of compound **1<sub>Dy</sub>** calculated on model 1-Dy.

Energy (cm <sup>-1</sup> )	$g_x$	$g_y$	$g_z$	Angle of $g_{zz}$ between ground and higher KDs (°)
0.00	0.10	0.32	19.08	—
48.32	0.27	0.44	18.41	90.34
97.38	2.86	3.30	12.94	27.85
131.85	8.05	5.61	3.09	35.07
177.76	1.84	2.99	12.68	85.88
240.39	0.09	0.25	16.73	87.57
322.36	0.21	1.40	17.34	50.14
333.79	0.16	1.59	17.75	86.74

Below are shown the results obtained for the equivalent excerpt of compound **1<sub>Dy</sub>** in which all coordinates have been taken from X-ray experiment, which has been named as model 2-Dy.

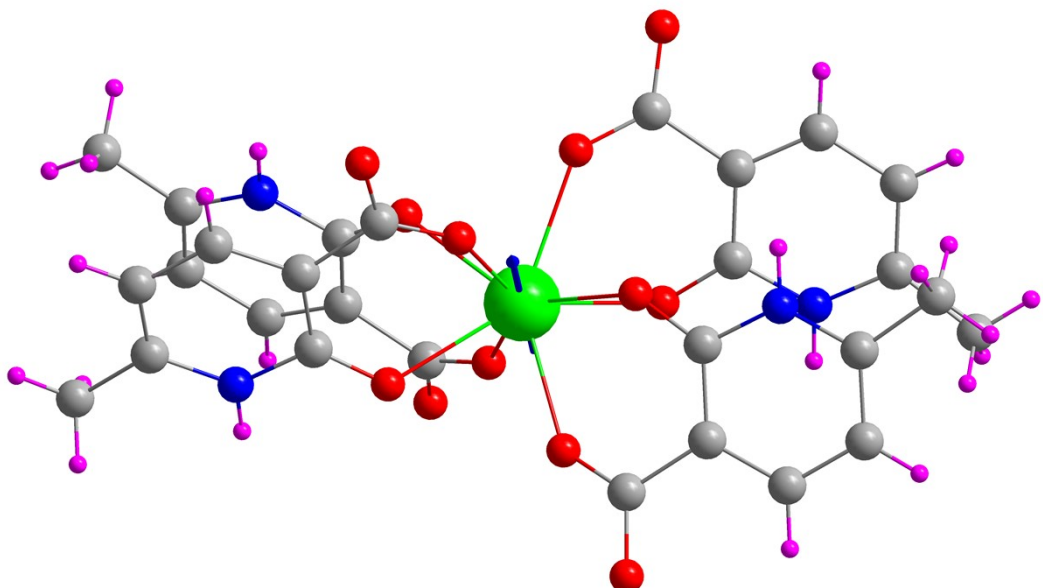


**Figure S21.** View of the Dy(III)-based model 2-Dy showing the main calculated magnetic axis of the ground state Kramers doublet.

**Table S4.** Energy spectrum and  $g$  tensors for the eight KDs arising from the GS of compound  $\mathbf{1}_{\text{Dy}}$  calculated on model 2-Dy.

Energy ( $\text{cm}^{-1}$ )	$g_x$	$g_y$	$g_z$	Angle of $g_{zz}$ between ground and higher KDs ( $^{\circ}$ )
0.00	0.08	0.23	19.25	—
55.91	0.32	0.40	18.62	89.98
106.09	3.03	3.65	12.83	22.21
142.73	3.27	5.40	8.47	90.92
193.00	1.55	2.45	13.04	87.20
263.85	0.05	0.19	16.77	88.68
341.34	0.14	0.33	18.97	50.51
363.42	0.08	0.46	19.26	90.15

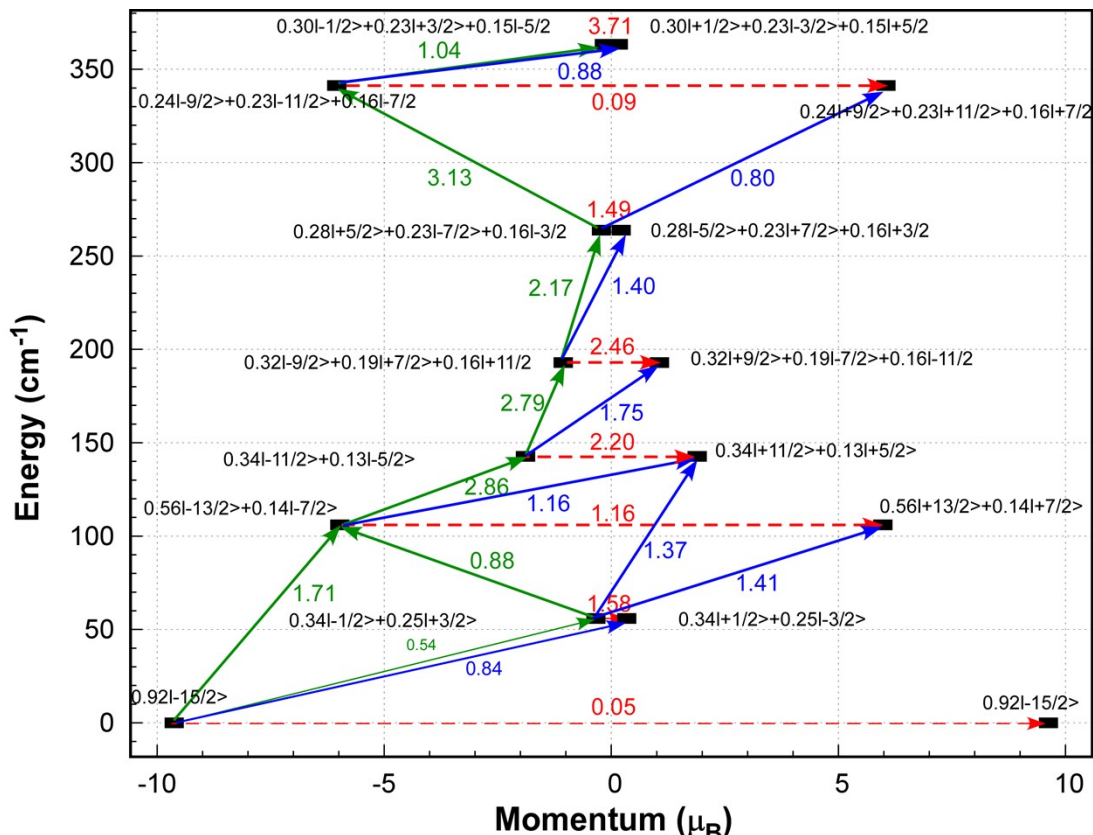


**Figure S22.** *Ab initio* computed relaxation mechanism showing the eight lowest KDs with the main wavefunctions on model 2-Dy (for compound  $\mathbf{1}_{\text{Dy}}$ ). Blue and green lines indicate the relaxation pathways for magnetization reversal mechanism through excited states. The dotted red lines represent the ground state QTM and TA-QTM via excited KDs. The numbers close to each arrow designate matrix elements of transition magnetic moment.

Below are shown the results obtained for an excerpt of compound **1<sub>Dy</sub>** consisting of the coordination fragment of the central Dy(III) ion and the four linked ligands as well as one of the two sodium ions with its complete coordination shell. All coordinates have been taken from X-ray experiment, although the hydrogen atoms have been optimized. This corresponds to model 3-Dy.

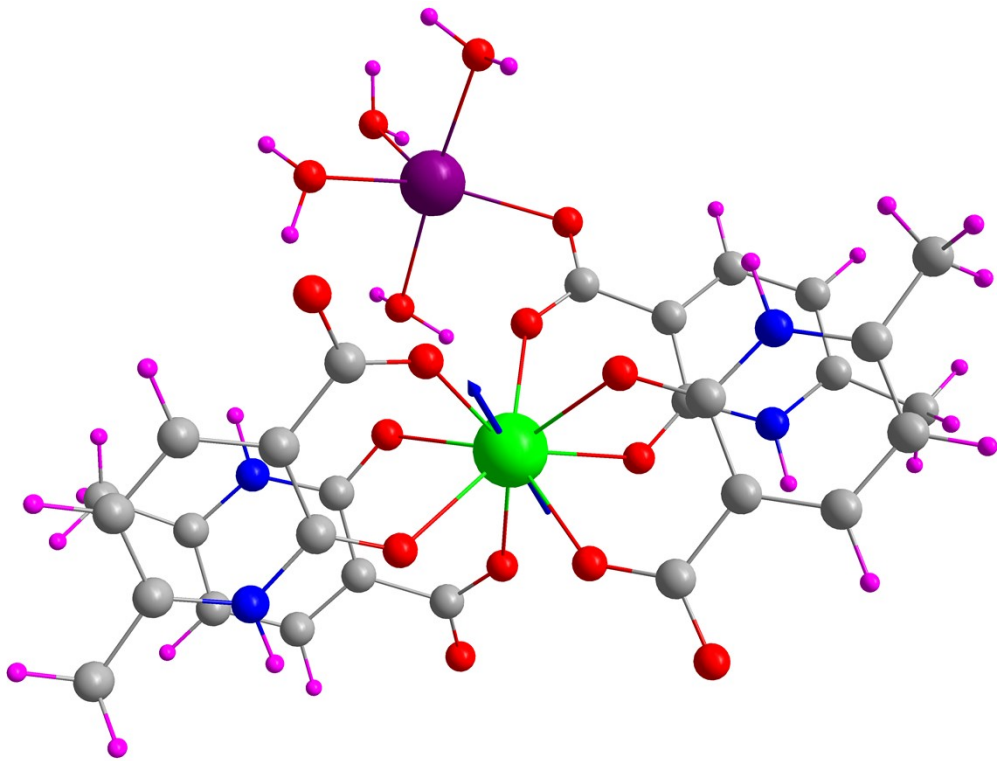
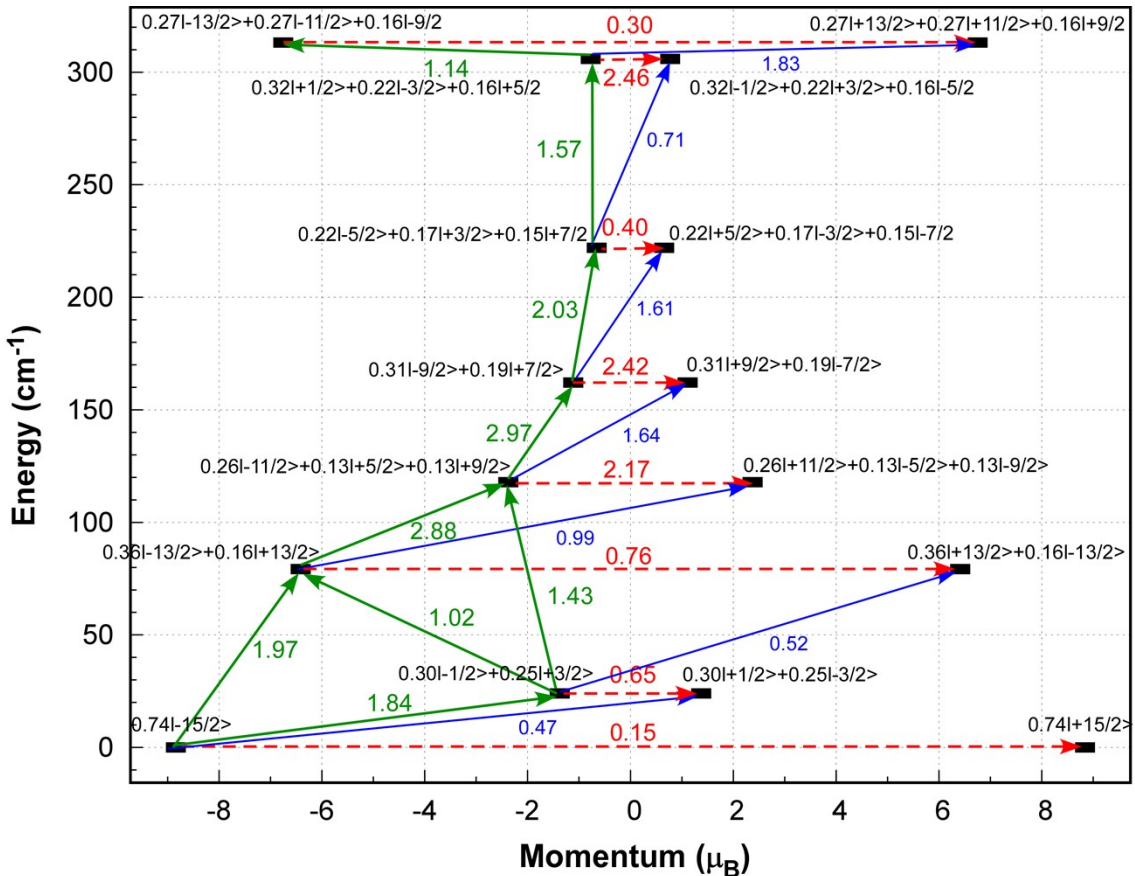


**Figure S23.** View of the Dy(III)-based model 3-Dy showing the main calculated magnetic axis of the ground state Kramers doublet.

**Table S5.** Energy spectrum and *g* tensors for the eight KDs arising from the GS of compound **1<sub>Dy</sub>** calculated on model 3-Dy.

Energy (cm <sup>-1</sup> )	<i>g</i> <sub>x</sub>	<i>g</i> <sub>y</sub>	<i>g</i> <sub>z</sub>	Angle of <i>g</i> <sub>zz</sub> between ground and higher KDs (°)
0.00	0.13	0.77	17.68	—
24.04	0.04	0.60	17.80	81.32
79.25	2.11	2.30	13.62	20.03
117.86	7.13	6.52	4.31	24.00
162.17	1.68	2.81	12.47	89.01
221.93	0.10	0.26	16.70	85.80
305.87	0.12	1.45	17.93	86.61
313.18	0.11	1.55	18.09	41.73



Below are shown the results obtained for an excerpt of compound **1<sub>Dy</sub>** consisting of the Dy(III)-based coordination fragment including the two sodium coordination environments. All coordinates have been taken from X-ray experiment, although the hydrogen atoms have been optimized. This corresponds to model 4-Dy.

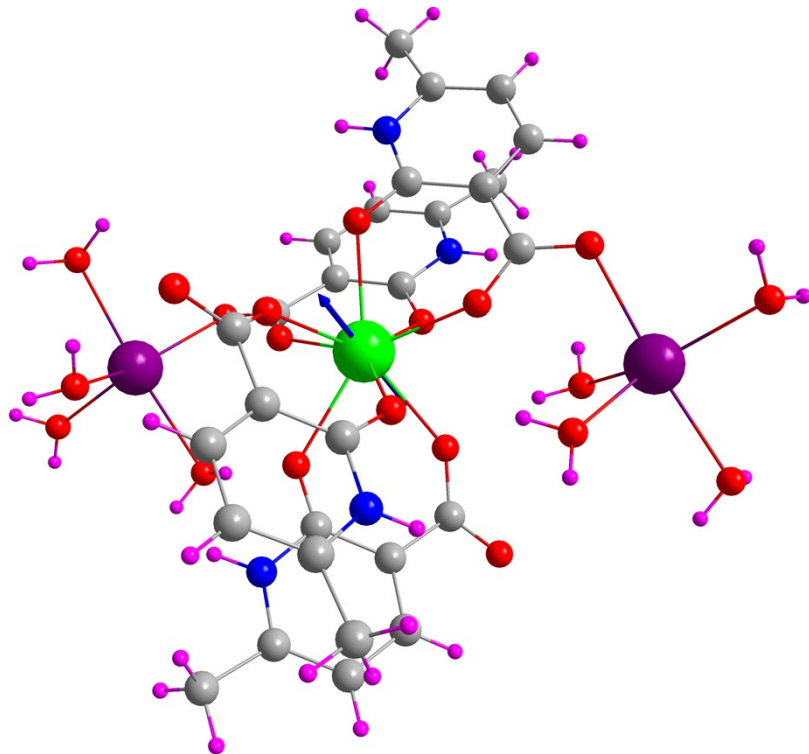


**Figure S25.** View of the Dy(III)-based model 4-Dy showing the main calculated magnetic axis of the ground state Kramers doublet.

**Table S6.** Energy spectrum and *g* tensors for the eight KDs arising from the GS of compound **1<sub>Dy</sub>** calculated on model 4-Dy.

Energy (cm <sup>-1</sup> )	<i>g</i> <sub>x</sub>	<i>g</i> <sub>y</sub>	<i>g</i> <sub>z</sub>	Angle of <i>g</i> <sub>zz</sub> between ground and higher KDs (°)
0.00	0.12	0.48	16.29	—
26.56	0.09	0.37	17.15	54.69
60.23	0.47	0.94	12.93	19.60
116.95	0.48	1.83	8.61	30.70
160.42	4.46	4.92	6.31	105.70
189.18	1.34	4.46	13.92	80.81
238.77	0.01	0.07	19.58	80.81
289.44	0.02	0.04	19.76	29.53

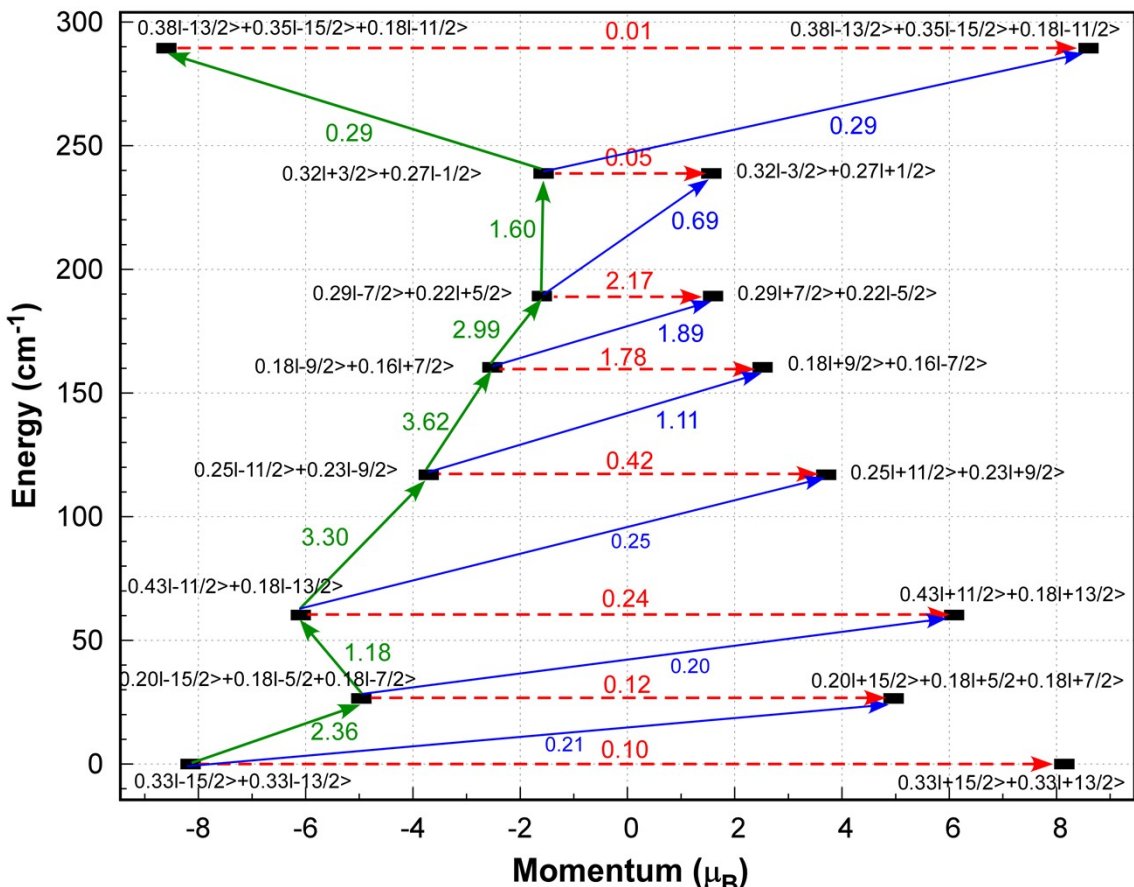


**Figure S26.** *Ab initio* computed relaxation mechanism showing the eight lowest KDs with the main wavefunctions on model 4-Dy (for compound  $\mathbf{1}_{\text{Dy}}$ ). Blue and green lines indicate the relaxation pathways for magnetization reversal mechanism through excited states. The dotted red lines represents the ground state QTM and TA-QTM via excited KDs. The numbers close to each arrow designate matrix elements of transition magnetic moment.

The large dependency of the low-lying KDs energy and admixture on the model implied suggests that their easy axes could be rotating one another. A detailed comparison of the easy axes of the ground and first excited states confirms that fact, as shown below. Among them, the switch is very evident not only between models 1-Dy and 2-Dy but also between 1-Dy and 4-Dy.

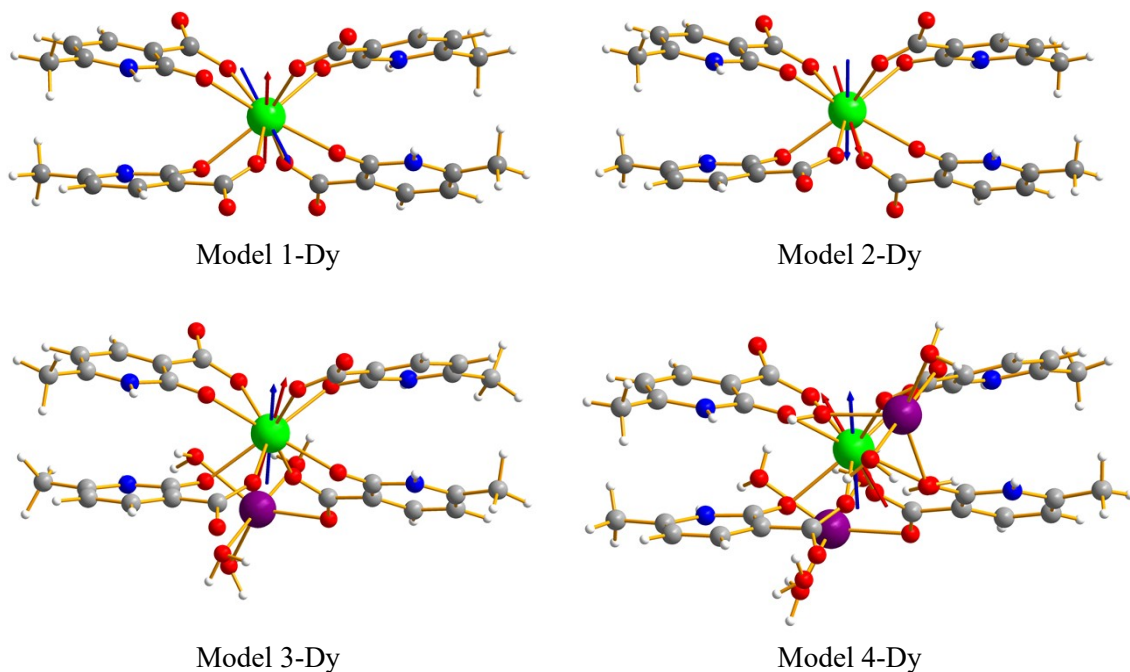


**Figure S27.** View of the easy axes of the ground (red arrow) and first excited (blue arrow) states directions projected on the Dy(III) atoms in the models.

Therefore, in an attempt to improve the results, another more sophisticated model based on the same excerpt of compound **1<sub>Dy</sub>** described in model 4-Dy but containing the point charges to simulate Madelung potential has been done, model 5-Dy hereafter. These results, shown below, reproduce fairly well the experimental results.

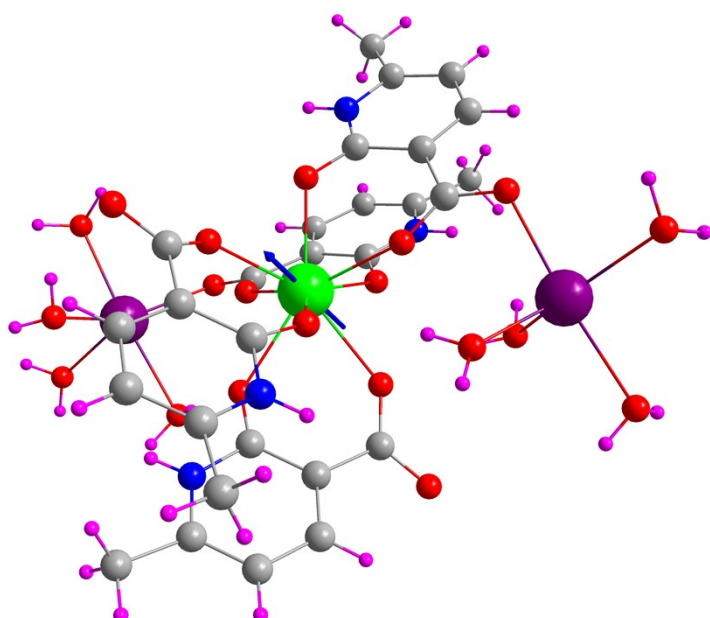


**Figure S28.** View of the Dy(III)-based model 5-Dy showing the main calculated magnetic axis of the ground state Kramers doublet.

**Table S7.** Energy spectrum and  $g$  tensors for the eight KDs arising from the GS of compound  $\mathbf{1}_{\text{Dy}}$  calculated on model 5-Dy.

Energy ( $\text{cm}^{-1}$ )	$g_x$	$g_y$	$g_z$	Angle of $g_{zz}$ between ground and higher KDs ( $^{\circ}$ )
0.00	0.17	0.32	18.54	—
31.87	0.05	0.42	15.32	41.09
74.95	0.68	1.31	13.22	26.55
128.42	0.96	2.82	8.56	29.71
173.18	3.59	4.91	6.81	77.00
203.16	1.46	4.65	13.98	70.53
258.28	0.01	0.07	19.53	70.51
301.72	0.03	0.07	19.70	31.12

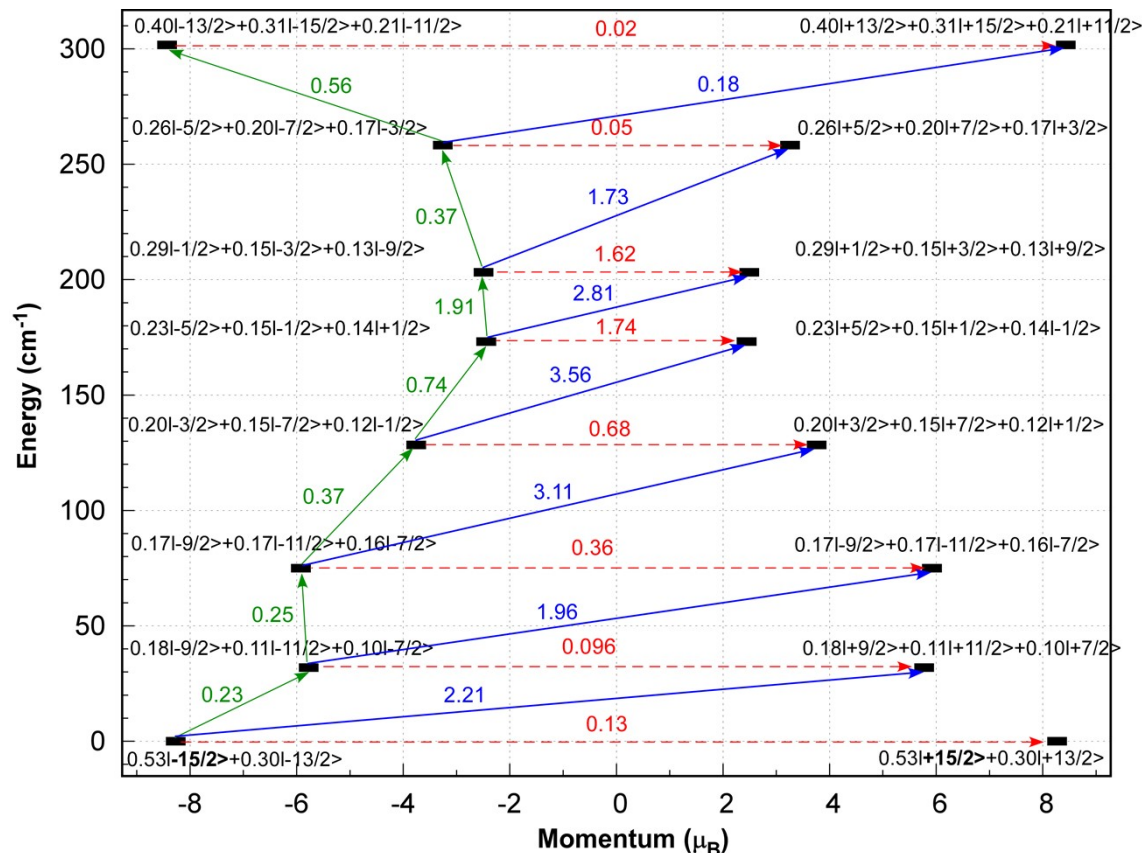


**Figure S29.** *Ab initio* computed relaxation mechanism showing the eight lowest KDs with the main wavefunctions on model 5-Dy (for compound  $\mathbf{1}_{\text{Dy}}$ ). Blue and green lines indicate the relaxation pathways for magnetization reversal mechanism through excited states. The dotted red lines represents the ground state QTM and TA-QTM via excited KDs. The numbers close to each arrow designate matrix elements of transition magnetic moment.

**Table S8.** Ab initio crystal-field parameters for model 1-Dy as defined by the crystal field hamiltonian.<sup>1</sup>

$k$	$q$	$\text{Re}(B_{kq})$	$\text{Im}(B_{kq})$	$ B_{kq} $	$k$	$q$	$\text{Re}(B_{kq})$	$\text{Im}(B_{kq})$	$ B_{kq} $
2	-2	6,173E+01	-1,246E+01	-2,91E-01	8	-8	-1,248E-03	-2,216E-02	-1,94E-08
2	-1	1,075E+01	4,062E+01	1,90E+00	8	-7	-2,535E-03	1,556E-02	5,44E-08
2	0	-8,732E+01	1,522E-15	-8,32E-01	8	-6	1,800E-02	5,379E-02	3,44E-08
2	1	-1,075E+01	4,062E+01	5,02E-01	8	-5	7,468E-02	-6,068E-03	-2,51E-08
2	2	6,173E+01	1,246E+01	1,44E+00	8	-4	9,312E-03	1,803E-02	1,04E-08
4	-4	5,922E+00	-2,570E+01	-1,31E-02	8	-3	1,732E-01	1,231E-01	1,82E-07
4	-3	-3,719E+01	-2,826E+01	-4,08E-02	8	-2	1,279E-01	-1,594E-01	-8,73E-08
4	-2	-5,330E+01	2,884E+01	1,11E-02	8	-1	1,215E-02	1,502E-02	1,96E-09
4	-1	1,375E+00	6,314E+00	3,45E-03	8	0	4,392E-01	-2,233E-17	3,39E-09
4	0	-6,052E+01	1,797E-15	-3,70E-03	8	1	-1,215E-02	1,502E-02	1,59E-09
4	1	-1,375E+00	6,314E+00	7,51E-04	8	2	1,279E-01	1,594E-01	7,00E-08
4	2	-5,330E+01	-2,884E+01	-2,06E-02	8	3	-1,732E-01	1,231E-01	2,57E-07
4	3	3,719E+01	-2,826E+01	-5,37E-02	8	4	9,312E-03	-1,803E-02	5,34E-09
4	4	5,922E+00	2,570E+01	3,02E-03	8	5	-7,468E-02	-6,068E-03	3,09E-07
6	-6	7,139E-01	3,193E+00	5,39E-05	8	6	1,800E-02	-5,379E-02	1,15E-08
6	-5	8,067E+00	4,417E+00	2,58E-04	8	7	2,535E-03	1,556E-02	-8,87E-09
6	-4	2,546E+00	-1,203E+01	-1,50E-04	8	8	-1,248E-03	2,216E-02	-1,09E-09
6	-3	-9,630E+00	-4,580E+00	-1,04E-04	10	-10	3,786E-03	-9,593E-04	-7,57E-11
6	-2	2,634E+00	-4,980E+00	-5,66E-05	10	-9	5,130E-03	-8,132E-03	-2,87E-09
6	-1	-1,826E+00	-4,046E+00	-5,82E-05	10	-8	-9,418E-03	-1,382E-02	-7,91E-10
6	0	-5,211E+00	-2,414E-16	-5,78E-06	10	-7	-1,906E-02	8,642E-03	1,21E-09
6	1	1,826E+00	-4,046E+00	-2,63E-05	10	-6	7,053E-03	1,894E-02	3,22E-10
6	2	2,634E+00	4,980E+00	3,00E-05	10	-5	4,659E-03	-3,041E-03	-9,25E-11
6	3	9,630E+00	-4,580E+00	-2,19E-04	10	-4	-8,327E-04	2,198E-02	1,06E-09
6	4	2,546E+00	1,203E+01	3,17E-05	10	-3	1,938E-02	7,380E-03	5,02E-10
6	5	-8,067E+00	4,417E+00	4,71E-04	10	-2	-3,000E-05	1,774E-02	1,18E-10
6	6	7,139E-01	-3,193E+00	1,20E-05	10	-1	1,412E-02	2,048E-02	1,58E-10
6	7	-1,826E+00	-4,046E+00	-5,82E-05	10	0	-1,885E-02	-3,478E-17	-6,92E-12
6	8	-5,211E+00	-2,414E-16	-5,78E-06	10	1	-1,412E-02	2,048E-02	1,09E-10
6	9	1,826E+00	-4,046E+00	-2,63E-05	10	2	-3,000E-05	-1,774E-02	-2,00E-13
6	10	2,634E+00	4,980E+00	3,00E-05	10	3	-1,938E-02	7,380E-03	1,32E-09
6	11	9,630E+00	-4,580E+00	-2,19E-04	10	4	-8,327E-04	-2,198E-02	-4,00E-11
6	12	2,546E+00	1,203E+01	3,17E-05	10	5	-4,659E-03	-3,041E-03	1,42E-10
6	13	-8,067E+00	4,417E+00	4,71E-04	10	6	7,053E-03	-1,894E-02	1,20E-10
6	14	7,139E-01	-3,193E+00	1,20E-05	10	7	1,906E-02	8,642E-03	-2,67E-09
6	15	-1,826E+00	-4,046E+00	-5,82E-05	10	8	-9,418E-03	1,382E-02	-5,39E-10
6	16	-5,211E+00	-2,414E-16	-5,78E-06	10	9	-5,130E-03	-8,132E-03	1,81E-09
6	17	1,826E+00	-4,046E+00	-2,63E-05	10	10	3,786E-03	9,593E-04	2,99E-10

**Table S9.** Ab initio crystal-field parameters for model 2-Dy as defined by the crystal field hamiltonian.<sup>1</sup>

$k$	$q$	$\text{Re}(B_{kq})$	$\text{Im}(B_{kq})$	$ B_{kq} $	$k$	$q$	$\text{Re}(B_{kq})$	$\text{Im}(B_{kq})$	$ B_{kq} $
2	-2	6,80E+01	-1,55E+01	-3,62E-01	8	-8	1,28E-03	-2,25E-02	-1,97E-08
2	-1	-1,17E+01	-4,35E+01	-2,03E+00	8	-7	4,30E-03	-1,80E-02	-6,29E-08
2	0	-1,01E+02	-4,23E-16	-9,58E-01	8	-6	1,47E-02	6,03E-02	3,85E-08
2	1	1,17E+01	-4,35E+01	-5,47E-01	8	-5	-7,70E-02	3,83E-03	1,59E-08
2	2	6,80E+01	1,55E+01	1,59E+00	8	-4	9,59E-04	3,30E-02	1,89E-08
4	-4	7,67E+00	-2,64E+01	-1,35E-02	8	-3	-1,94E-01	-1,47E-01	-2,18E-07
4	-3	3,81E+01	3,14E+01	4,54E-02	8	-2	1,33E-01	-1,61E-01	-8,79E-08
4	-2	-5,51E+01	2,83E+01	1,09E-02	8	-1	-3,32E-02	-6,38E-02	-8,34E-09
4	-1	-3,20E-01	-2,47E+00	-1,35E-03	8	0	4,79E-01	8,97E-17	3,69E-09
4	0	-6,36E+01	3,51E-16	-3,88E-03	8	1	3,32E-02	-6,38E-02	-4,35E-09
4	1	3,20E-01	-2,47E+00	-1,75E-04	8	2	1,33E-01	1,61E-01	7,28E-08
4	2	-5,51E+01	-2,83E+01	-2,13E-02	8	3	1,94E-01	-1,47E-01	-2,88E-07
4	3	-3,81E+01	3,14E+01	5,51E-02	8	4	9,59E-04	-3,30E-02	5,51E-10
4	4	7,67E+00	2,64E+01	3,92E-03	8	5	7,70E-02	3,83E-03	-3,19E-07
6	-6	2,22E-01	3,69E+00	6,22E-05	8	6	1,47E-02	-6,03E-02	9,39E-09
6	-5	-8,35E+00	-5,15E+00	-3,01E-04	8	7	-4,30E-03	-1,80E-02	1,51E-08
6	-4	3,26E+00	-1,28E+01	-1,59E-04	8	8	1,28E-03	2,25E-02	1,12E-09
6	-3	9,03E+00	4,74E+00	1,08E-04	10	-10	4,48E-03	-8,86E-05	-6,99E-12
6	-2	3,30E+00	-5,51E+00	-6,26E-05	10	-9	-7,13E-03	8,24E-03	2,91E-09
6	-1	1,89E+00	4,41E+00	6,35E-05	10	-8	-8,75E-03	-1,64E-02	-9,38E-10
6	0	-4,90E+00	1,38E-16	-5,44E-06	10	-7	2,16E-02	-7,94E-03	-1,11E-09
6	1	-1,89E+00	4,41E+00	2,72E-05	10	-6	6,26E-03	2,03E-02	3,45E-10
6	2	3,30E+00	5,51E+00	3,76E-05	10	-5	-3,13E-03	2,90E-03	8,83E-11
6	3	-9,03E+00	4,74E+00	2,05E-04	10	-4	-1,58E-03	2,46E-02	1,18E-09
6	4	3,26E+00	1,28E+01	4,06E-05	10	-3	-1,67E-02	-7,61E-03	-5,17E-10
6	5	8,35E+00	-5,15E+00	-4,88E-04	10	-2	-3,95E-03	2,29E-02	1,53E-10
6	6	2,22E-01	-3,69E+00	3,75E-06	10	-1	-1,33E-02	-2,17E-02	-1,67E-10
					10	0	-2,37E-02	-1,19E-18	-8,69E-12
					10	1	1,33E-02	-2,17E-02	-1,02E-10
					10	2	-3,95E-03	-2,29E-02	-2,63E-11
					10	3	1,67E-02	-7,61E-03	-1,13E-09
					10	4	-1,58E-03	-2,46E-02	-7,59E-11
					10	5	3,13E-03	2,90E-03	-9,51E-11
					10	6	6,26E-03	-2,03E-02	1,06E-10
					10	7	-2,16E-02	-7,94E-03	3,03E-09
					10	8	-8,75E-03	1,64E-02	-5,01E-10
					10	9	7,13E-03	8,24E-03	-2,52E-09
					10	10	4,48E-03	8,86E-05	3,53E-10

**Table S9.** Ab initio crystal-field parameters for model 3-Dy as defined by the crystal field hamiltonian.<sup>1</sup>

$k$	$q$	$\text{Re}(B_{kq})$	$\text{Im}(B_{kq})$	$ B_{kq} $	$k$	$q$	$\text{Re}(B_{kq})$	$\text{Im}(B_{kq})$	$ B_{kq} $
2	-2	-1,27E+01	-2,24E+00	-5,23E-02	8	-8	9,74E-02	-1,58E-02	-1,39E-08
2	-1	-1,73E+01	4,23E+01	1,97E+00	8	-7	3,66E-02	-2,01E-02	-7,02E-08
2	0	1,47E+02	-1,19E-15	1,40E+00	8	-6	-8,13E-03	-2,17E-02	-1,39E-08
2	1	1,73E+01	4,23E+01	-8,05E-01	8	-5	9,03E-02	8,20E-02	3,39E-07
2	2	-1,27E+01	2,24E+00	-2,97E-01	8	-4	-1,69E-02	-4,43E-02	-2,54E-08
4	-4	6,81E+01	-2,66E+00	-1,36E-03	8	-3	1,12E-01	6,78E-02	1,00E-07
4	-3	2,42E+01	-2,74E+01	-3,95E-02	8	-2	-2,21E-02	-4,46E-02	-2,44E-08
4	-2	-4,44E+01	4,81E+00	1,86E-03	8	-1	-2,10E-01	5,01E-03	6,55E-10
4	-1	-2,92E+01	-1,28E+01	-6,97E-03	8	0	9,65E-02	2,60E-16	7,44E-10
4	0	1,85E+01	1,04E-15	1,13E-03	8	1	2,10E-01	5,01E-03	-2,75E-08
4	1	2,92E+01	-1,28E+01	-1,60E-02	8	2	-2,21E-02	4,46E-02	-1,21E-08
4	2	-4,44E+01	-4,81E+00	-1,72E-02	8	3	-1,12E-01	6,78E-02	1,65E-07
4	3	-2,42E+01	-2,74E+01	3,49E-02	8	4	-1,69E-02	4,43E-02	-9,70E-09
4	4	6,81E+01	2,66E+00	3,48E-02	8	5	-9,03E-02	8,20E-02	3,74E-07
6	-6	1,55E+00	-5,64E+00	-9,52E-05	10	-10	6,60E-03	-1,69E-02	-1,33E-09
6	-5	5,16E+00	1,43E+01	8,38E-04	10	-8	1,23E-02	1,04E-02	5,94E-10
6	-4	-5,45E-01	2,66E+00	3,31E-05	10	-7	-6,51E-03	-7,72E-03	-1,08E-09
6	-3	-4,72E+00	1,87E-01	4,26E-06	10	-6	3,18E-03	-4,18E-04	-7,10E-12
6	-2	4,96E+00	-1,12E+00	-1,27E-05	10	-5	3,40E-03	4,98E-03	1,52E-10
6	-1	3,63E+00	-5,08E+00	-7,31E-05	10	-4	4,14E-03	1,39E-02	6,67E-10
6	0	-1,21E+00	4,24E-16	-1,35E-06	10	-3	-1,44E-02	-9,71E-03	-6,60E-10
6	1	-3,63E+00	-5,08E+00	5,22E-05	10	-2	-8,79E-03	4,60E-04	3,06E-12
6	2	4,96E+00	1,12E+00	5,64E-05	10	-1	3,28E-02	4,05E-03	3,12E-11
6	3	4,72E+00	1,87E-01	-1,07E-04	10	0	-6,21E-03	-1,63E-17	-2,28E-12
6	4	-5,45E-01	-2,66E+00	-6,79E-06	10	1	-3,28E-02	4,05E-03	2,52E-10
6	5	-5,16E+00	1,43E+01	3,02E-04	10	2	-8,79E-03	-4,60E-04	-5,86E-11
6	6	1,55E+00	5,64E+00	2,62E-05	10	3	1,44E-02	-9,71E-03	-9,82E-10
					10	4	4,14E-03	-1,39E-02	1,99E-10
					10	5	-3,40E-03	4,98E-03	1,03E-10
					10	6	3,18E-03	4,18E-04	5,41E-11
					10	7	6,51E-03	-7,72E-03	-9,12E-10
					10	8	1,23E-02	-1,04E-02	7,04E-10
					10	9	-9,12E-03	2,41E-02	3,22E-09
					10	10	6,60E-03	1,69E-02	5,21E-10

**Table S10.** Ab initio crystal-field parameters for model 4-Dy as defined by the crystal field hamiltonian.<sup>1</sup>

$k$	$q$	$\text{Re}(B_{kq})$	$\text{Im}(B_{kq})$	$ B_{kq} $	$k$	$q$	$\text{Re}(B_{kq})$	$\text{Im}(B_{kq})$	$ B_{kq} $
2	-2	4,63E+01	2,85E+00	6,65E-02	8	-8	9,71E-04	3,53E-02	3,09E-08
2	-1	-3,96E+00	-2,11E+01	-9,83E-01	8	-7	1,08E-02	-1,73E-02	-6,04E-08
2	0	-5,67E+01	1,54E-15	-5,40E-01	8	-6	2,71E-02	2,75E-02	1,76E-08
2	1	3,96E+00	-2,11E+01	-1,85E-01	8	-5	4,74E-02	8,99E-02	3,72E-07
2	2	4,63E+01	-2,85E+00	1,08E+00	8	-4	-2,90E-03	2,04E-02	1,17E-08
4	-4	-6,40E+00	6,07E+00	3,10E-03	8	-3	2,27E-02	-1,65E-02	-2,44E-08
4	-3	-3,30E+01	-6,84E+00	-9,88E-03	8	-2	3,14E-02	2,19E-01	1,20E-07
4	-2	-3,24E+01	-5,69E+01	-2,20E-02	8	-1	-2,05E-01	3,59E-01	4,70E-08
4	-1	3,31E+01	-3,70E+01	-2,02E-02	8	0	3,70E-02	2,69E-16	2,85E-10
4	0	-4,47E+01	1,77E-15	-2,73E-03	8	1	2,05E-01	3,59E-01	-2,68E-08
4	1	-3,31E+01	-3,70E+01	1,80E-02	8	2	3,14E-02	-2,19E-01	1,72E-08
4	2	-3,24E+01	5,69E+01	-1,25E-02	8	3	-2,27E-02	-1,65E-02	3,36E-08
4	3	3,30E+01	-6,84E+00	-4,77E-02	8	4	-2,90E-03	-2,04E-02	-1,66E-09
4	4	-6,40E+00	-6,07E+00	-3,27E-03	8	5	-4,74E-02	8,99E-02	1,96E-07
6	-6	4,58E+00	1,75E+00	2,96E-05	8	6	2,71E-02	-2,75E-02	1,73E-08
6	-5	1,89E+00	-1,54E-01	-9,00E-06	8	7	-1,08E-02	-1,73E-02	3,79E-08
6	-4	-4,84E+00	6,69E+00	8,33E-05	8	8	9,71E-04	-3,53E-02	8,49E-10
6	-3	-1,69E+01	-3,25E+00	-7,39E-05	10	-10	-2,12E-03	1,02E-03	8,03E-11
6	-2	9,48E-01	-7,48E+00	-8,51E-05	10	-9	-5,63E-03	-3,20E-03	-1,13E-09
6	-1	-2,51E+00	7,40E-01	1,06E-05	10	-8	-1,73E-03	-5,33E-03	-3,05E-10
6	0	-4,90E+00	1,19E-15	-5,44E-06	10	-7	2,94E-03	-5,58E-03	-7,82E-10
6	1	2,51E+00	7,40E-01	-3,62E-05	10	-6	1,72E-02	2,99E-03	5,08E-11
6	2	9,48E-01	7,48E+00	1,08E-05	10	-5	6,33E-03	2,46E-02	7,49E-10
6	3	1,69E+01	-3,25E+00	-3,85E-04	10	-4	-1,42E-02	5,05E-03	2,43E-10
6	4	-4,84E+00	-6,69E+00	-6,03E-05	10	-3	3,03E-02	5,50E-03	3,74E-10
6	5	-1,89E+00	-1,54E-01	1,10E-04	10	-2	7,16E-03	4,36E-02	2,91E-10
6	6	4,58E+00	-1,75E+00	7,72E-05	10	-1	-7,82E-03	-1,56E-02	-1,20E-10
					10	0	2,33E-02	-2,31E-17	8,56E-12
					10	1	7,82E-03	-1,56E-02	-6,02E-11
					10	2	7,16E-03	-4,36E-02	4,78E-11
					10	3	-3,03E-02	5,50E-03	2,06E-09
					10	4	-1,42E-02	-5,05E-03	-6,84E-10
					10	5	-6,33E-03	2,46E-02	1,92E-10
					10	6	1,72E-02	-2,99E-03	2,92E-10
					10	7	-2,94E-03	-5,58E-03	4,12E-10
					10	8	-1,73E-03	5,33E-03	-9,88E-11
					10	9	5,63E-03	-3,20E-03	-1,99E-09
					10	10	-2,12E-03	-1,02E-03	-1,67E-10

**Table S11.** Ab initio crystal-field parameters for model 5-Dy as defined by the crystal field hamiltonian.<sup>1</sup>

$k$	$q$	$\text{Re}(B_{kq})$	$\text{Im}(B_{kq})$	$ B_{kq} $	$k$	$q$	$\text{Re}(B_{kq})$	$\text{Im}(B_{kq})$	$ B_{kq} $
2	-2	5,16E+01	-2,17E+00	-5,07E-02	8	-8	1,28E-02	1,19E-02	1,04E-08
2	-1	-1,96E+00	-8,78E+00	-4,09E-01	8	-7	-2,67E-02	-6,16E-04	-2,15E-09
2	0	-2,93E+01	4,55E-16	-2,79E-01	8	-6	-7,11E-03	8,66E-03	5,53E-09
2	1	1,96E+00	-8,78E+00	-9,15E-02	8	-5	4,46E-02	5,25E-03	2,17E-08
2	2	5,16E+01	2,17E+00	1,20E+00	8	-4	-1,45E-02	-3,16E-02	-1,81E-08
4	-4	-1,53E+00	-5,62E+00	-2,87E-03	8	-3	-5,61E-02	-1,10E-01	-1,64E-07
4	-3	-1,95E+00	-1,91E+01	-2,77E-02	8	-2	-3,15E-02	-4,82E-02	-2,64E-08
4	-2	2,75E+01	-3,79E+01	-1,46E-02	8	-1	-3,40E-01	5,68E-02	7,43E-09
4	-1	6,64E+01	-4,54E+01	-2,48E-02	8	0	-5,57E-01	1,35E-16	-4,30E-09
4	0	5,02E+00	-1,94E-16	3,07E-04	8	1	3,40E-01	5,68E-02	-4,45E-08
4	1	-6,64E+01	-4,54E+01	3,62E-02	8	2	-3,15E-02	4,82E-02	-1,72E-08
4	2	2,75E+01	3,79E+01	1,06E-02	8	3	5,61E-02	-1,10E-01	-8,31E-08
4	3	1,95E+00	-1,91E+01	-2,82E-03	8	4	-1,45E-02	3,16E-02	-8,32E-09
4	4	-1,53E+00	5,62E+00	-7,82E-04	8	5	-4,46E-02	5,25E-03	1,85E-07
6	-6	4,70E+00	-1,18E+00	-1,99E-05	8	6	-7,11E-03	-8,66E-03	-4,54E-09
6	-5	-1,18E+00	-8,14E-01	-4,76E-05	8	7	2,67E-02	-6,16E-04	-9,35E-08
6	-4	-2,88E+00	-4,01E+00	-5,00E-05	8	8	1,28E-02	-1,19E-02	1,12E-08
6	-3	2,80E-02	-5,40E+00	-1,23E-04	10	-10	-9,09E-04	-1,50E-03	-1,18E-10
6	-2	7,52E+00	-1,27E+01	-1,45E-04	10	-9	-9,28E-04	-2,69E-03	-9,48E-10
6	-1	8,68E+00	3,15E+00	4,54E-05	10	-8	7,90E-04	-3,31E-03	-1,90E-10
6	0	-1,24E+01	-8,21E-17	-1,38E-05	10	-7	-2,18E-03	3,07E-03	4,30E-10
6	1	-8,68E+00	3,15E+00	1,25E-04	10	-6	-8,04E-03	-1,43E-04	-2,42E-12
6	2	7,52E+00	1,27E+01	8,56E-05	10	-5	-1,37E-02	-7,05E-03	-2,14E-10
6	3	-2,80E-02	-5,40E+00	6,36E-07	10	-4	-6,28E-03	-9,21E-03	-4,43E-10
6	4	-2,88E+00	4,01E+00	-3,59E-05	10	-3	-4,51E-03	-6,47E-03	-4,40E-10
6	5	1,18E+00	-8,14E-01	-6,91E-05	10	-2	-3,14E-03	1,54E-02	1,02E-10
6	6	4,70E+00	1,18E+00	7,94E-05	10	-1	-7,78E-02	5,39E-02	4,15E-10
					10	0	-1,10E-02	-3,02E-18	-4,04E-12
					10	1	7,78E-02	5,39E-02	-5,99E-10
					10	2	-3,14E-03	-1,54E-02	-2,09E-11
					10	3	4,51E-03	-6,47E-03	-3,07E-10
					10	4	-6,28E-03	9,21E-03	-3,02E-10
					10	5	1,37E-02	-7,05E-03	-4,16E-10
					10	6	-8,04E-03	1,43E-04	-1,37E-10
					10	7	2,18E-03	3,07E-03	-3,05E-10
					10	8	7,90E-04	3,31E-03	4,52E-11
					10	9	9,28E-04	-2,69E-03	-3,27E-10
					10	10	-9,09E-04	1,50E-03	-7,17E-11

In the following figures and table it is described the main results obtained for an excerpt of compound  $\mathbf{2}_{\text{Er}}$  consisting of the metal ion and the four coordinated ligands. Hydrogen atoms have been optimized for this excerpt, so it has named model 5-Er for consistency with the Dy-based model.

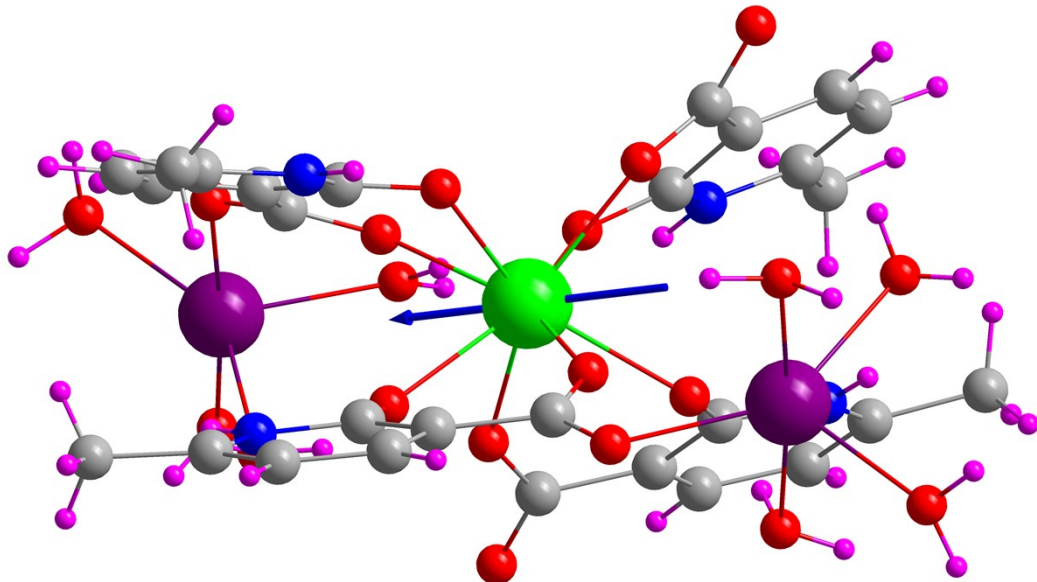


**Figure S30.** View of the Er(III)-based model 5-Er showing the main calculated magnetic axis of the ground state Kramers doublet (GSKD).

**Table S7.** Energy spectrum and  $g$  tensors for the eight KDs arising from the GS of compound  $\mathbf{2}_{\text{Er}}$  calculated on model 5-Er).

Energy ( $\text{cm}^{-1}$ )	$g_x$	$g_y$	$g_z$	Angle of $g_{zz}$ between ground and higher KDs ( $^{\circ}$ )
0.00	0.67	2.54	15.18	—
63.12	3.02	5.18	8.95	98.40
80.13	0.94	2.21	14.73	90.86
94.20	0.91	3.49	9.78	95.58
161.13	0.02	3.01	6.22	94.21
187.65	0.44	0.52	12.96	100.92
228.69	0.71	2.08	9.78	114.50
253.42	0.09	0.61	13.48	56.03

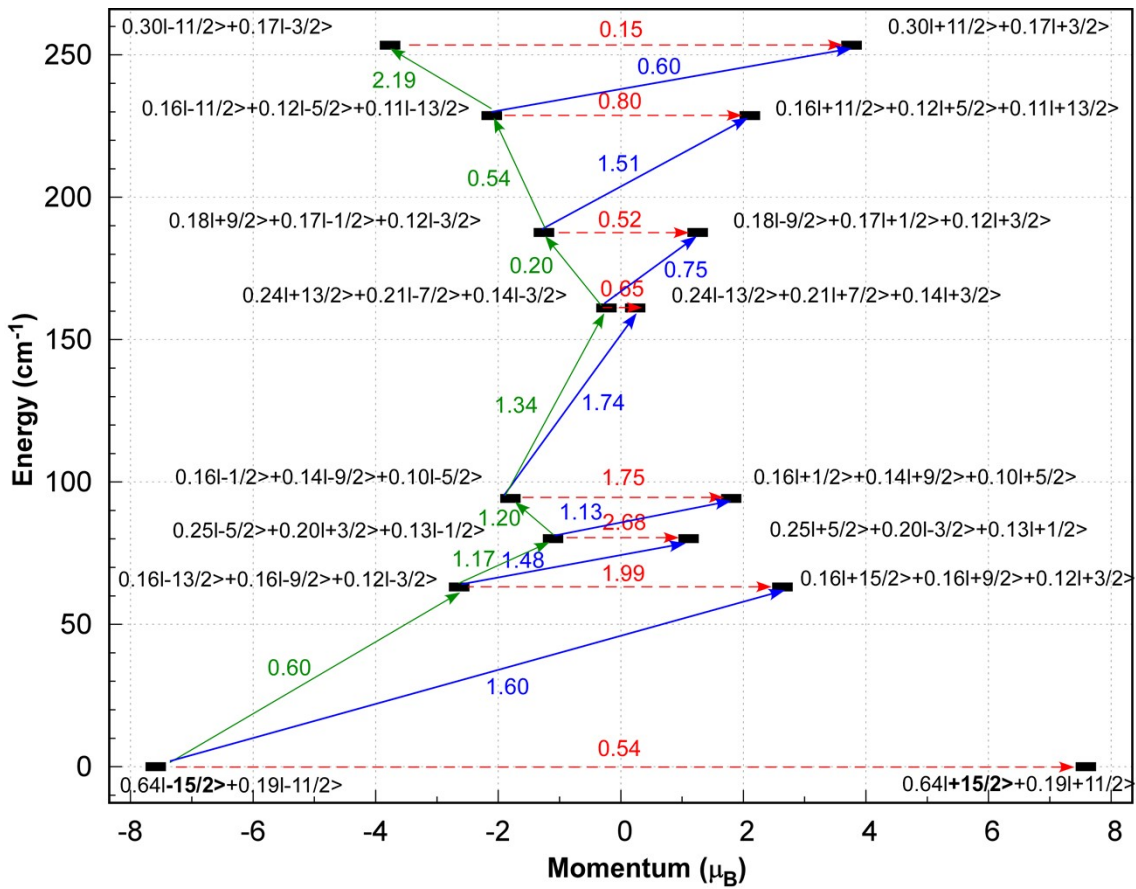


**Figure S31.** *Ab initio* computed relaxation mechanism showing the eight lowest KDs with the main wavefunctions on model 1-Er (for compound  $2_{\text{Er}}$ ). Blue and green lines indicate the relaxation pathways for magnetization reversal mechanism through excited states. The dotted red lines represents the ground state QTM and TA-QTM via excited KDs. The numbers close to each arrow designate matrix elements of transition magnetic moment.

**Table S11.** Ab initio crystal-field parameters for model 5-Er as defined by the crystal field hamiltonian.<sup>1</sup>

$k$	$q$	$\text{Re}(B_{kq})$	$\text{Im}(B_{kq})$	$ B_{kq} $	$k$	$q$	$\text{Re}(B_{kq})$	$\text{Im}(B_{kq})$	$ B_{kq} $
2	-2	-1,04E+01	4,63E+00	1,08E-01	8	-8	2,07E-02	-8,52E-04	-7,45E-10
2	-1	-1,03E+01	-3,45E+00	-1,61E-01	8	-7	-1,12E-03	5,71E-04	2,00E-09
2	0	-2,96E+01	-2,79E-16	-2,82E-01	8	-6	-5,51E-03	-4,99E-04	-3,19E-10
2	1	1,03E+01	-3,45E+00	-4,78E-01	8	-5	-2,49E-03	-3,94E-03	-1,63E-08
2	2	-1,04E+01	-4,63E+00	-2,43E-01	8	-4	4,10E-02	1,29E-03	7,43E-10
4	-4	-4,90E+01	3,82E+00	1,95E-03	8	-3	-1,96E-02	1,28E-03	1,90E-09
4	-3	2,02E-01	-3,76E+00	-5,43E-03	8	-2	4,40E-02	-1,61E-02	-8,81E-09
4	-2	3,29E+01	4,08E+00	1,58E-03	8	-1	-3,37E-03	8,70E-04	1,14E-10
4	-1	5,05E+00	2,21E+00	1,21E-03	8	0	2,10E-03	1,43E-17	1,62E-11
4	0	-3,63E+01	-1,74E-16	-2,22E-03	8	1	3,37E-03	8,70E-04	-4,41E-10
4	1	-5,05E+00	2,21E+00	2,76E-03	8	2	4,40E-02	1,61E-02	2,41E-08
4	2	3,29E+01	-4,08E+00	1,27E-02	8	3	1,96E-02	1,28E-03	-2,91E-08
4	3	-2,02E-01	-3,76E+00	2,92E-04	8	4	4,10E-02	-1,29E-03	2,35E-08
4	4	-4,90E+01	-3,82E+00	-2,50E-02	8	5	2,49E-03	-3,94E-03	-1,03E-08
6	-6	1,38E+01	3,64E-01	6,14E-06	8	6	-5,51E-03	4,99E-04	-3,52E-09
6	-5	1,16E+01	-9,41E-01	-5,50E-05	8	7	1,12E-03	5,71E-04	-3,93E-09
6	-4	-1,98E+01	1,73E+00	2,15E-05	8	8	2,07E-02	8,52E-04	1,81E-08
6	-3	5,50E+00	6,32E-01	1,44E-05	10	-10	-3,06E-03	1,98E-04	1,57E-11
6	-2	2,15E+01	3,40E+00	3,86E-05	10	-9	-4,11E-04	1,53E-04	5,39E-11
6	-1	3,26E+00	-2,10E-01	-3,02E-06	10	-8	2,32E-03	2,10E-04	1,20E-11
6	0	-1,38E+01	1,61E-16	-1,53E-05	10	-7	1,66E-03	2,24E-04	3,15E-11
6	1	-3,26E+00	-2,10E-01	4,69E-05	10	-6	2,55E-03	1,28E-05	2,18E-13
6	2	2,15E+01	-3,40E+00	2,45E-04	10	-5	-7,21E-04	1,76E-04	5,34E-12
6	3	-5,50E+00	6,32E-01	1,25E-04	10	-4	6,72E-03	-5,10E-04	-2,45E-11
6	4	-1,98E+01	-1,73E+00	-2,47E-04	10	-3	1,51E-03	-5,67E-04	-3,86E-11
6	5	-1,16E+01	-9,41E-01	6,80E-04	10	-2	-1,22E-02	6,67E-04	4,45E-12
6	6	1,38E+01	-3,64E-01	2,34E-04	10	-1	-2,42E-03	-1,82E-04	-1,40E-12
					10	0	1,13E-02	-5,74E-18	4,15E-12
					10	1	2,42E-03	-1,82E-04	-1,87E-11
					10	2	-1,22E-02	-6,67E-04	-8,11E-11
					10	3	-1,51E-03	-5,67E-04	1,03E-10
					10	4	6,72E-03	5,10E-04	3,23E-10
					10	5	7,21E-04	1,76E-04	-2,19E-11
					10	6	2,55E-03	-1,28E-05	4,33E-11
					10	7	-1,66E-03	2,24E-04	2,32E-10
					10	8	2,32E-03	-2,10E-04	1,33E-10
					10	9	4,11E-04	1,53E-04	-1,45E-10
					10	10	-3,06E-03	-1,98E-04	-2,41E-10

**S7. Additional figures of the crystal structure.**

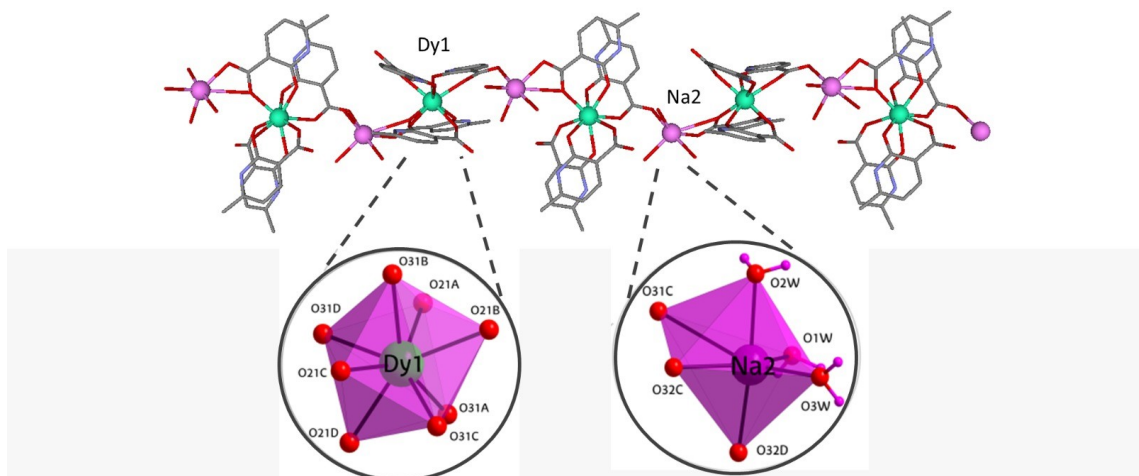


**Figure S32.** View of the metal-organic chain of compound  $\mathbf{1}_{\text{Dy}}$ .

## **S8. References.**

- 1 L. Gu and R. Wu, *Phys. Rev. B*, 2021, **103**, 014401.